CHALMERS
UNIVERSITY OF TECHNOLOGY

Influence of inhibitors on the hydrolysis of spruce residues

For the production of bioethanol

Master's thesis in biotechnology

DAVID SUNDBERG

Department of biology and biological engineering
CHALMERS UNIVERSITY OF TECHNOLOGY
Gothenburg, Sweden 2018

Influence of Inhibitors on the Hydrolysis of Spruce Residues

For the Production of Bioethanol

DAVID SUNDBERG

Department of biology and biological engineering
CHALMERS UNIVERSITY OF TECHNOLOGY
Gothenburg, Sweden 2018

Influence of Inhibitors on Hydrolysis of Spruce Residues
For the Production of Bioethanol
DAVID SUNDBERG

Supervisor: David Benjamin Nickel, Industrial Biotechnology
Examiner: Carl Johan Franzén, Industrial Biotechnology

Master's Thesis 2018: October
Department of biology and biological engineering
Chalmers University of Technology
SE-412 96 Göteborg
Sweden
Telephone + 46 (0)31-772 1000

Influence of Inhibitors on Hydrolysis of Spruce Residues
For the Production of Bioethanol

DAVID SUNDBERG
Department of biology and biological engineering
Chalmers University of Technology

ABSTRACT

Sustainable fuel ethanol may be produced from lignocellulosic materials such as wood and straw. The use of forestry residues may allow for bioethanol to be produced in a sustainable way. However, very little systematic work has been performed on the pretreatment, hydrolysis and fermentation of forest residues. Utilizing forest residues would increase the value of forest products, contribute to the development of a circular economy and combat climate change by diminishing the need for fossil fuels in the transportation sector. In this project, the inhibitory effect on the enzymes responsible for glucose release from Norway spruce (*Picea abies*) residues from branches, tips and needles during enzymatic hydrolysis have been investigated. Inhibitors native to the material and produced during the pretreatment increases the process cost and diminishes yields for bioethanol production.

An anaerobic parallel shake flask system for performing the hydrolysis has been developed and assembled. The material has been both chemically and physically characterized, and method development for analysis of pretreated and hydrolyzed material using high performance liquid chromatography and ion chromatography has been done.

Method development using a Kinetex F5 Core-shell LC column, Rezex™ RPM-Monosaccharide Pb+2 (8%) column, and a Rezex™ ROA-Organic Acid H+ (8%), 150 x 7.8 mm LC column has laid a foundation for future method development that might result in large time savings for the analysis of both pretreated and hydrolyzed spruce residue material. The holocellulosic fractions of the material were consistent with the literature. It was concluded that mild pretreatment conditions were likely to produce the highest amount of releasable sugars. Nevertheless, the materials were quite recalcitrant, and only about 30% of the theoretical glucose yield on cellulose was achieved. Despite some indications that increased ethanol and acetate concentrations in the hydrolysate decreases the hydrolysis rate and yield respectively it is likely that increasing inhibitor concentrations within realistic spans do not affect productivity and yield significantly.

Keywords: Bioethanol, Inhibition, Hydrolysis, *Picea abies*

Contents

List of abbreviations

Table 1 – Abbreviations used in this thesis.

Abbreviation	Word/Term
ACN	Acetonitrile
ARGM	Arabinose, rhamnose, galactose and mannose
FPU	Filter Paper Units
HMF	5-(hydroxymethyl)-furfural
HPLC	High-performance liquid chromatography
IC	Ion chromatography
PDA	Photo diode array
RI	Refractive index
SSCF	Simultaneous saccharification and co-fermentation
UV/VIS	Ultraviolet-Visible Spectroscopy
WIS	Water insoluable solids
YPD	Yeast peptone dextrose
RISE	Research Institute of Sweden
NADH	Nicotinamide adenine dinucleotide

Introduction

In this section, the scientific background and theory will be covered. The aim and scope of the project will also be detailed.

Background

Anthropogenic climate change has over the last 70 years caused major changes to the planet's climate: Increased atmospheric and ocean temperatures, melting ice caps and sea level rise which threaten many unique ecosystems, the security of coastal regions and diminishing agricultural yields for our most important crops [1, 2]. The cause for climate change is largely attributed to human emissions of greenhouse gases into the atmosphere from the burning of fossil fuels [2].

Researchers and policy-makers are working to develop sustainable alternatives to replace the use of fossil fuels [2]. Biofuels are one such group of alternatives which could be used in the transportation sector. Examples of these include bioethanol, biodiesel and biogas [3-5]. Biodiesel dominated biofuels globally in 2010, followed by bioethanol with a 17% volumetric share of global biofuel production, corresponding to 86 billion liters or 2800 ktoe [3-5]. Today, bioethanol is produced from agricultural products and residues. As shown by Wang et al. and Borrion et al., greenhouse gas emissions can be significantly reduced by using bioethanol compared to conventional gasoline [6, 7]. Since it utilizes existing refueling infrastructure and technology, bioethanol is an appealing alternative fuel. Bioethanol can be produced from different sugar sources and depending on the source the ethanol is classified as either first or second generation biofuel. First generation biofuels are produced from sources commonly rich in starch such as sugar canes, rice, corn and potatoes [8-10].

Policy makers fear however that using food crops for biofuel production might inflate food prices, although the science on the matter does not show concrete evidence for this proposition [11-14]. There is therefore a growing interest in second generation bioethanol which instead uses wood, wood residues and other agricultural residues such as wheat straw as substrates [10, 15]. Wood and wood residues are lignocellulosic materials, which dry weight consist mostly of the cell wall, which in turn consists of up to 75% polysaccharides [16]. Lignocellulosic materials thus hold a large potential for being utilized as a feedstock for fermentative bioethanol production. Cellulose is one of the most common polymers in lignocellulosic material together with the amorphous polymer hemicellulose and the polyaromatic lignin [10, 17]. Cellulose is a sturdy, crystalline glucose polymer while hemicellulose consists of a heterogeneous mixture of monomer sugars, usually with a backbone of xylan or galactoglucomannan with side chains of galactose, arabinose, rhamnose, mannose and other sugars [10, 17]. There are however important differences between lignocellulosic materials. In softwood the concentration of xylose for example is lower than in hardwood [18]. Both hardwood and softwood lignin contains guaiacyl and syringyl units, but softwood contains fewer syringyl units [18, 19]. This makes lignin in softwood more stable under acid conditions compared to hardwood. [18].

Table 2 – Mass of sugars and polysaccharides in different parts of spruce wood. Values are listed in mg/g dried wood or bark.

	Cellulose	Hemicellulose	Glucose	Xylose	Mannose
Sapwood[20]	466	195	35.0	57.3	94.2
Heartwood[20]	440	195	30.6	59.8	86.2
Inner bark[21]	225	266	75	25	13
Outer bark[21]	107	228	46	45	22
Stem wood[22]	420	273			
Bark[22]	266	92			
Branches[22]	290	300			
Needles[22]	282	254			

The polysaccharide content of different parts of the softwood Norway spruce, *Picea abies*, has been investigated in previous studies [20-24]. Willför et al. characterized stem wood, both heart wood and sapwood for non-cellulosic polysaccharides, cellulose, and water soluble saccharides [20]. They identified glucose, mannose, xylose, galactose, rhamnose, arabinose, glucuronic acid, galacturonic acid and 4-O-methyl-glucuronic acid [20]. Mannose was the most common monomer sugar in hemicellulose followed by xylose [20]. Krogell et al. investigated the composition of inner and outer bark in Norway spruce [21]. The polysaccharides identified were the same as in the study by Willför et. al [20, 21]. Glucose was the overwhelmingly most common monomer in inner bark while being in a slight majority in outer bark followed by xylose in both cases [21]. Cellulose made up 22.5 mass percent (m/m = m%) and 10.7m% for inner and outer bark respectively, but older sources have found values even lower [21, 23, 24]. Räisänen et al. have documented the composition of stem wood, bark, branches and needles in Norway spruce [22]. According to the data, cellulose content is highest in stem wood and lower in branches, needles, and bark respectively [22]. The hemicellulose concentration is however highest in branches and lower in stem wood, needles, and bark respectively [22].

A comparison of the data from Willför et.al, Krogel et. al and Räisänen et al. can be found in Table 2. The amount of polysaccharides differs significantly between different parts of the tree but also between studies. Räisänen et al. reported higher hemicellulose content in stem wood compared with Willför et al. and higher cellulose content but much lower hemicellulose content in bark than Krogell et al. [20-22]. Cellulose is dominating in stem wood while hemicellulose is more common in branches and needles [20, 22]. It is important to understand the composition and characteristics of the specific material to be able to develop an efficient process for the production of bioethanol. However, knowing the composition and characteristics of the untreated material is not sufficient. The specifics of the process design for bioethanol production will change the material throughout. This means that it is also of great importance to understand the effects of each unit operation on the material. The composition of a mixture of Norway spruce residues has yet to be investigated.

An overview of a possible production process can be seen in Figure 1. The lignocellulosic material is first pretreated. Steam explosion with sulfuric acid or sulfur dioxide, also known as

acid catalyzed steam explosion, is one of the most widely used physico-chemical pretreatments for lignocellulosic materials [25]. The lignin is separated out and the remaining slurry is enzymatically hydrolyzed to produce monosaccharides. The sugars are then fermented to produce CO_2 and ethanol, where the latter is distilled to be used as a fuel for transportation.

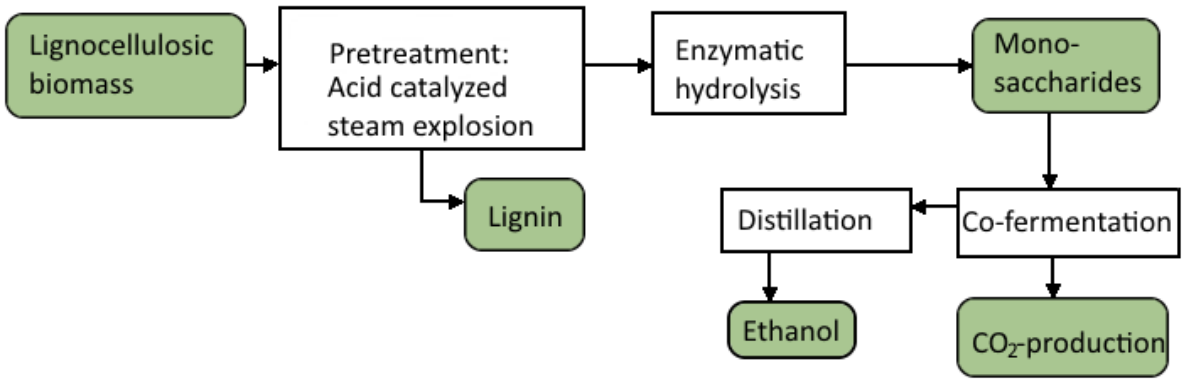

Figure 1 – Overview of a hypothetical biorefinery process of lignocellulosic material for the main production of bioethanol. Secondary production streams of lignin could be used to produce natural binders and adhesives while the CO_2 produced during fermentation could be used as supercritical CO_2 and be used in chemical extraction plants.

The pretreatment process for second generation substrates has been investigated to improve effectiveness and efficiency. Talebnia et al. has found that sugar yields of up to 99.6% and ethanol yields of up to 99.0% compared to their respective theoretical maximal value are achievable in wheat straw [26]. But it was also concluded that there is no optimal pretreatment method as of now [26]. Alvira et al. have identified low temperatures, the avoidance of milling and grinding before pretreatment, using as small pretreatment reactors as justifiable, and having low moisture content as important parameters for an energy-efficient pretreatment [25]. The pretreatment should also be designed so that lignin recovery is possible and that a minimal amount of solid bio-waste is produced [25]. Furthermore, the process should produce monosaccharides or short oligosaccharides in high concentrations, but avoid sugar or lignin degradation into inhibitors [25]. This is important to ensure both high product yields and high survivability of the fermenting yeast [25]. The pretreatment should also be tailored to generate sugar profiles that are compatible with the fermentative capabilities of the yeast, which is important with respect to pentoses such as xylose and arabinose [25]. The pentoses pose a problem as non-engineered *S. cerevisiae* cannot ferment them [27]. However, genetically engineered strains are able to ferment both pentoses and hexoses, called co-fermentation, using both ideal feedstocks and realistic lignocellulosic materials [11, 27, 28].

During acid catalyzed steam explosion the material is heated to high temperatures and pressurized for up to a few minutes followed by rapidly depressurized of the reactor [25]. This causes rapid auto-hydrolysis of the hemicellulose and disintegration of the material [25]. The structural removal of the hemicellulose increases cellulose accessibility for the enzymes and increases pore size [25]. Small pore sizes has been determined to be the main factor for lower hydrolysis rates because small pores trap the enzymes [25]. The steam explosion also removes

and redistributes some of the lignin [10]. Because the hemicellulose and lignin are decomposed into smaller pieces they can be more easily separated into a liquid fraction [10]. The crystalline cellulose however is sturdier and some of it will remain solid until subject to the enzymatic treatment where it is hydrolyzed into glucose [10].

Steam explosion has several advantages compared to other pretreatments such as using less hazardous chemicals, its feasibility to be industrially implemented and the ability to use larger wood chip sizes, thus eliminating excessive grinding and milling [25]. Steam explosion has been proven useful for poplar, olive residues, herbaceous residues and wheat straw and it has been demonstrated to be one of the most effective strategies for softwoods [25]. A drawback is the production of degradation products [25]. These consist of aromatic furan derivatives such as furfural and HMF which are formed from incomplete sugar degradation. HMF is derived from the degradation of hexoses while furfural is derived from pentoses. Furthermore, weak organic acids are produced such as acetic acid, formic acid, levulinic acid as well as lignin derivatives [10, 25]. Acetic acid is derived from the acetyl groups of the hemicellulose while formic and levulinic acid are further degradation products of HMF [25].

Several aspects of the material have been investigated for their effect on the hydrolysis and the following fermentation into bioethanol [25, 26, 29-31]. Increasing degree of cellulose crystallinity will decrease the rate of hydrolysis [29]. The lignin will provide a physical barrier as well as act as a site for enzyme to bind unspecifically [25]. The waxy outside of tree bark also hinders enzyme to reach the cellulose and must be addressed in the pretreatment [25]. The differences in structure of the cellulose and hemicellulose require complex enzymatic mixtures which makes the choice of enzymes important [26]. The presence of pretreatment and hydrolysis products as well as degradation products such as aromatics, organic acids and lignin can contribute to lowering the effective activity of any enzymes added or might work toxic against the fermenter, which is usually *S. cerevisiae* [26, 30, 31]. Some of the inhibitors are indigenous in the material, while some are produced during pretreatment of the material [25, 30].

Second generation bioethanol is currently not commercially viable. This is not due to a lack of substrate availability, which are cheap and readily available, but rather in part because of the technical barriers in the pretreatment and hydrolysis process described previously to lower the costs of bioethanol production to make it commercially viable several parts of the process needs to be focused on [10]. These include: Lowering the energy requirements of the pretreatment, improving the cellulose and hemicellulose conversion rate into monomeric carbohydrates, develop industrial scale processes with the ability to co-ferment both hexoses and pentoses, manage to extract and process the lignin into other useful chemical products, lowering enzyme costs, and minimizing the influence of inhibitors [10].

Aims and scope

This thesis is intended to contribute to a fundamental understanding of inhibitory action during hydrolysis to enable production of bioethanol from Norway spruce residues using *S. cerevisiae* as the fermenter. More specifically, this project has aimed to generate knowledge

about the composition of tips, needles and branches from Norway spruce as well as inhibitor profiles for the same material pretreated using acid catalyzed steam explosion. A lab-scale hydrolysis process has been developed to study inhibitory action on hydrolysis. Furthermore, analysis method development for the detection of inhibitors and hydrolysis products has been investigated. The objective was to develop a faster analysis method for hydrolysate samples.

Several research questions have been attempted to be answered along with the insights aspired to be reached and mentioned in the above paragraph. Are there any indications that effects of the inhibitors can be grouped for modelling purposes and if so, what indications? Do the results call for any special considerations for a future simultaneous saccharification and co-fermentation (SSCF) process, and if so, how? What are important blind spots in this project which needs to be addressed or acknowledged when moving forward? To address these questions, the glucose production rate during hydrolysis was explored under different inhibition loading scenarios.

Methods & materials

This chapter contains the chemicals and materials used as well as the methods applied to perform the different experiments. All dilutions in this report are reported in the form 1:x, where x is the fractional concentration of the stock concentration listed in Table 11 in the appendix. As an example, a 1:3 solution has one third the concentration of the stock concentration.

Chemicals

All chemicals used are listed in Table 3. All solid chemicals used were anhydrous unless otherwise noted. The spruce residues were obtained from the Biorefinery Demo Plant in Örnsköldsvik, Sweden.

Standards and stocks

All standards and stocks prepared and used extensively throughout this project are listen in Table 11 the appendix. All standards and stocks were weighed into 50 mL falcon tubes and diluted to 45 mL with MilliQ water. They were stored frozen at -20 °C when not needed.

Analysis methods

Water insoluble solids determination

Water insoluble solid (WIS) determination was performed on the pretreated material as well as on the endpoint samples of hydrolysate slurry. Samples were washed with MilliQ water and centrifuged consecutively using the Avanti J-26S XP Beckman coulter centrifuge at 8000 rpm for 20 min at 4 °C until the glucose concentration in the supernatant was below 50 mg/L. The supernatant was removed between each centrifugation. The glucose concentration was measured using MQuant glucose test strips from Merck Millipore.

Weighed aluminum dishes were dried at 105 °C in a BINDER drying and heating chamber overnight. 2 g of wet solid hydrolysate from each sample was placed in the aluminum dish and dried at 105 °C overnight. The dried material was weighed and frozen to be used for two-step acid hydrolysis, as previously described, in the future. The WIS was calculated by dividing the product between the mass of the washed wet solids and the mass of the dried solids with the product between the original mass of the wet slurry and the mass of the washed wet slurry added to the aluminum dish.

Table 3 – List of all chemicals used during this project.

Chemical name	CAS-number	Manufacturer
Sulfuric Acid	7664-93-9	EMSURE® Merck Millipore
Calcium carbonate	471-34-1	EMSURE® Merck Millipore
D-Glucose	50-99-7	Formedium™
D-Xylose	58-86-6	Sigma Aldrich
D-Galactose	59-23-4	Sigma Aldrich
L-Arabinose	5328-37-0	Biochemica, Applichem
D-Mannose	3458-28-4	Sigma Aldrich
Rhamnose	3615-41-6	Sigma Aldrich
Sodium acetate	127-09-3	Sigma Aldrich
Trisodium citrate dihydrate	6132-04-3	Sigma Aldrich
Trans-ferulic acid	537-98-4	Sigma Aldrich
Ferulic acid	1135-24-6	Apin Chemicals Ltd.
Levulinic acid	123-76-2	Sigma Aldrich
Ethanol	64-17-5	BDH Chemicals, VWR
Glycerol	56-81-5	BDH Chemicals, VWR
5-(hydroxymethyl)furfural (HMF)	67-47-0	Sigma Aldrich
Furfural	98-01-1	Sigma Aldrich
Vanillin	121-33-5	Sigma Aldrich
Formic acid	64-18-6	EMSURE® Merck Millipore
3,5-dinitrosalicylic acid	609-99-4	Sigma Aldrich
Potassium sodium tartrate tetrahydrate	304-59-6	Sigma Aldrich
Phenol	108-95-2	Merck, VWR international
Sodium metabisulfite	7681-57-4	Sigma Aldrich
Sodium hydroxide	1310-73-2	BDH Chemicals, VWR
Citric acid monohydrate	77-92-9	Sigma Aldrich
Hydrochloric acid	7647-01-0	EMSURE® Merck Millipore
Cellic CTec2	50-99-7	Sigma Aldrich
Nitrogen gas	7727-37-9	N/A
Phosphoric acid	7664-38-2	Sigma Aldrich
Acetonitrile	75-05-8	Sigma Aldrich
Methanol	67-56-1	BDH Chemicals, VWR
Sorbic acid	110-44-1	Sigma Aldrich

High-performance liquid chromatography

High-performance liquid chromatography (HPLC) was used to quantify acids, aromatics as well as glucose, ethanol and glycerol in pretreated material and in hydrolysate slurry. The analytes were separated and detected on a Jasco Extreme system running ChromNav CFR Ver.2.01.7 build 6, LC-4000 with a BS-400-1 Bottle stand, an AS-4150 RHPLC Autosampler, a PU-4180 RHPLC Pump, a CO-4061 Column oven, an UV-4075 UV/VIS detector, a RI-4030 refractive index (RI) detector and a LC-NetII/ADC interface box using a Rezex™ ROA-Organic Acid H+ (8%), 150 x 7.8 mm LC column running each sample for 45 min with an injection volume of 5 µL 5 mM H_2SO_4 at 80 °C with a mobile phase speed of 0.8 mL min^{-1}. Detection was made with the UV/VIS detector at 210 nm and the RI detector. HPLC standards used with the pretreated material were glucose (25 g L^{-1}), galactose (25 g L^{-1}), mannose (25 g L^{-1}), xylose (25 g L^{-1}), ethanol (25 g L^{-1}), glycerol (5 g L^{-1}), 5-(hydroxymethyl)furfural (HMF) (10 g L^{-1}), furfural (10 g L^{-1}), vanillin (2.5 g L^{-1}), levulinic acid (2.5 g L^{-1}), acetate (12.5 g L^{-1}), citrate (15 g L^{-1}), formic acid (5 g L^{-1}), ferulic acid (0.5 g L^{-1}), and trans-ferulic acid (0.5 g L^{-1}). The standards were run in a binary dilution series from 1:1 to 1:64 dilutions and were made with MilliQ water. HPLC standards used with the hydrolysate include the above mentioned standards with the same dilutions except vanillin, ferulic acid and trans-ferulic acid which were not used.

HPLC method development was conducted to analyze inhibitor samples faster and more precise. As opposed to the characterization of the material, the method development was carried out using the above mentioned column and HPLC system, although not together. A Kinetex F5 Core-shell LC column, a Rezex™ RPM-Monosaccharide Pb+2 (8%) column and another HPLC system with the same hardware and software as mentioned in the previous paragraph but with an MD-4010 Photo diode array (PDA) detector instead of the UV/VIS detector and RI detector was also used. The two HPLC systems will here forth be referred to as the isocratic HPLC and the gradient HPLC respectively as the latter was set up to run gradients and mixed mobile phases while the former was not. The three columns used will hereby be referenced as the Rezex ROA, Kinetex F5 and Rezex Pb columns. Standards used during the HPLC method development were the same as mentioned above, with the exception of vanillin, ferulic and trans-ferulic acid which were not used arabinose (25 g L^{-1}), rhamnose (25 g L^{-1}) and sorbic acid (1.5 g L^{-1}) which were used. Dilutions used are specified in Table 13-15 in the appendix and were made with MilliQ water.

Sixteen experiments were conducted using the Kinetex F5 column on the gradient HPLC that are detailed in Table 13 in the appendix. The first experiments were based on the protocol for detecting food additives available in the technical information for the column [32]. Isocratic and gradient methods were performed using 0.1v% phosphoric acid or MilliQ water together with acetonitrile (ACN). A near optimum ratio (±10%) between the two liquid phases was determined as well as near optimum detection wavelengths (±10 nm). A hydrolysis sample was run and peak detection was applied. Calibration curves for HMF and Furfural were done. The objective was to develop a faster analysis method for hydrolysate samples.

Twelve experiments were conducted using the Rezex Pb column on the isocratic HPLC that are detailed in Table 14 in appendix for the detection of monosaccharides and alcohols (ethanol and glycerol). First experiments were based on the method developed by McGinley [33]. Different flow rates, temperatures and mobile phases were tested. Mobile phases tested were MilliQ water, 0.4v% MeOH diluted in MilliQ water, 4v% MeOH diluted in MilliQ water and 4v% ACN diluted in MilliQ water. Calibration series for glucose, xylose, mannose, rhamnose, arabinose, galactose, ethanol, glycerol and the new sugar mix were made and run. The objective was to find a replacement analysis method for the use of ion chromatography (IC).

Five experiments were conducted using the Rezex ROA column on the gradient HPLC that are detailed in Table 15 in appendix. The method was based on the same method used on isocratic HPLC. Sugar, acid and aromatic mixes were run as well as one hydrolysate sample, the acid single standards and HMF and furfural. The objective was to develop a method on a second HPLC system to allow for parallel analysis and thereby shorten analysis duration.

Ion chromatography

IC was performed using a Dionex ICS-3000 Reagent-Free™ IC system running Chromeleon™ Chromatography Data System for the characterization of the pretreated slurry. IC standards used with the pretreated material were sorbitol (100 mg L^{-1}), mannitol (100 mg L^{-1}), arabinose (100 mg L^{-1}), rhamnose (100 mg L^{-1}), galactose (100 mg L^{-1}), glucose (100 mg L^{-1}), xylose (100 mg L^{-1}), mannose (100 mg L^{-1}) and fructose (9 mg L^{-1}). Dilutions of IC standards were made with 10 mg L^{-1} fructose solution, which served as an internal standard. The liquid fraction samples were run together with a binary dilution series of the sorbitol, mannitol, arabinose, rhamnose, galactose, glucose, and xylose standards at dilutions 1:1 to 1:128 and the mannose standard at dilutions 1:1 to 1:16 (see Table 11 in the appendix). The solid fraction samples were run together with a binary dilution series of the sorbitol, mannitol, arabinose, rhamnose, galactose, glucose, and xylose standards at dilutions 1:1 to 1:32 and the mannose standard at dilutions 1:1 to 1:16 (see Table 11 in the appendix). The recovery standards used with the solid fraction were mannose (340 mg L^{-1}), galactose (173 mg L^{-1}), glucose (1384 mg L^{-1}), xylose (208 mg L^{-1}), and arabinose (92 mg L^{-1}) and were run at 1:50 dilution.

Determination of compositional & physical characteristics of spruce residues

Prior to this project, Norway spruce residues from branches, tips and needles had been pretreated using 1 L kg^{-1} 4m% sulfuric acid and steam explosion in accordance with a design of experiments plan. The pretreatment experiments were performed by Emma Johansson at the Research Institute of Sweden (RISE) Processum, Örnsköldsvik. This has resulted in thirteen different batches of pretreated slurry that were frozen. See Table 4 which presents an overview of these batches. The temperature and residence time in the reactor were design variables in a central composite design.

Table 4 – Overview of the thirteen different batches of pretreatment material. The rows 'Temperature' to 'Severity factor' describe the parameters included in the experimental design of pretreatments performed on the spruce residues. The severity factor is a quantity that relates biomatrix opening to pH, temperature and holding time of the pretreatment [34]. The WIS listed is the mass percentage of water insoluble solids in the material after pretreatment.

Material ID	MAT.IB.100	MAT.IB.101	MAT.IB.102	MAT.IB.103	MAT.IB.104	MAT.IB.105
Temperature (°C)	204	214	211	214	204	204
Time (min)	20	20	4.4	7	7	7
Severity factor	4.36	4.66	3.91	4.20	3.91	3.91
WIS (m%)	14.49	13.87	15.10	13.11	17.17	16.91
Material ID	**MAT.IB.106**	**MAT.IB.107**	**MAT.IB.108**	**MAT.IB.109**	**MAT.IB.110**	**MAT.IB.111**
Temperature (°C)	209	209	209	209	200	206
Time (min)	13.5	13.5	13.5	13.5	13.5	13.5
Severity factor	4.34	4.34	4.34	4.34	4.07	4.25
WIS (m%)	14.18	13.77	15.73	15.89	18.68	17.55
Material ID	**MAT.IB.112**					
Temperature (°C)	213					
Time (min)	22.6					
Severity factor	4.68					
WIS (m%)	12.51					

The pretreated slurry was separated by centrifugation at 9000 rpm for 25 min using an Avanti J-26S XP Beckman coulter centrifuge into two fractions, a liquid fraction and a solid fraction. The liquid fraction was filtered from any particulates while the wet solids were washed and dried in accordance with the methodology for WIS determination. Excess dried solids were stored at -20 °C until further analysis. The measured WIS for each pretreatment batch can be seen in Table 4.

In this project, triplicate sample of the liquid fraction were prepared and analyzed using IC to identify the sugars, and HPLC to identify the inhibitors. The solid fraction was hydrolyzed and the fraction of polysaccharides was calculated according to A. Sluiter, et al. by two-step sulfuric acid hydrolysis [35]. The generated sugar monomers were measured in tri- or hexaplicates using IC.

For the liquid fraction analysis on the IC, each sample was diluted 1:10 into a 10 mg L^{-1} fructose solution. Proteins were removed by heating each sample to 100°C for 1h on a heating block to precipitate them and filtered out with a 25 mm w/ 0.2 µm PTFE membrane syringe filter prior to analysis. The samples were further diluted to 1:500 into the 10 mg L^{-1} fructose solution. The samples were run on the IC together with the standards according to the analysis method section. For the liquid fraction analysis on the HPLC, each sample was diluted 1:3 with MilliQ water. The samples were then filtered through 0.2 µm nylon filters. The samples were run on the HPLC together with the standards according to the analysis method section.

The solids were powdered using a Qiagen TissueLyser II and weighed into samples á 60 mg and dried overnight at 105 °C. 600 µL of 12 M sulfuric acid was added to each sample. The

samples were put in a 30 °C water bath under stirring at 150 rpm. During incubation, every 20 minute the samples were vortexed briefly. After 60 min, 16.8 mL of MilliQ water was added. The samples were autoclaved at 121 °C for 1h together with the recovery standards, which were processed to quantify the sugar loss throughout the two-step hydrolysis. After cooling, solid $CaCO_3$ was then added to neutralize the acid. The samples were diluted to 1:50 using 50 mg L^{-1} fructose and centrifuged at 5000 rpm for 5 min at 4 °C. They were then filtered through 25 mm w/ 0.2 µm PTFE membrane syringe filters. Lastly, the samples and the sugar recovery standards were heated for 10 min at 90 °C before being analyzed together with the standards according to the analysis method section. The amount of cellulose and hemicellulose present in the dried, pretreated slurry was then determined using the results from the IC analysis of the solid fraction. Below the equation used for calculating the polymeric sugars from the monomer data is presented:

$$C_{polymer,j} = \frac{1}{n} \sum_{i=1}^{n} C_{Data,i,j} * R_j * A_{Corr,j} * \frac{V}{m_{i,j}} \qquad (1)$$

Where $C_{polymer,j}$ is the concentration of polymeric sugar *j* expressed as a mass fraction (mass polymeric sugar per mass solids in pretreated slurry), *n* is the number of replicates for each pretreatment sample set, $C_{Data,i,j}$ is the concentration of the monomeric sugar as determined by the IC analysis, R_j is the recovery rate for sugar *j*, $A_{Corr,j}$ is the anhydrous correction term for sugar *j* which is listed in Table 5, *V* is the total volume of the hydrolysis reaction, i.e. 17.346 mL, and $m_{i,j}$ is the weighed mass of water insoluble solids used in the two-step hydrolysis process for each replicate *i* and each sugar *j*.

Table 5 – The anhydrous correction terms for each of the monosaccharides used during characterization of the solid fraction. The term is an empirical fraction between the mass of the polymeric sugar per sugar unit and the mass of the monomer sugar.

Sugar	Anhydrous Correction term
Arabinose	0.88
Galactose	0.9
Glucose	0.9
Xylose	0.88
Mannose	0.9

Liquid fraction density determination

Pretreated slurry was thawed and adjusted to pH 5.00 using 2 M NaOH. Two 50 mL falcon tubes containing 25.96 g and 25.94 g of pH-adjusted slurry were prepared. 1122 µL of 1 M citrate buffer and 1353 µL of Cellic CTec2 (LOT # SLBS6227) diluted 1:10 in MilliQ water was added to each sample. The samples were then centrifuged at 5000 rpm for 20 min at 30 °C. The supernatant was then transferred to a new set of falcon tubes and centrifuged again under the same conditions. The volume and mass of the liquid of two replicates was then measured and the average density calculated.

Enzymatic assay for activity determination

An enzymatic assay was performed to determine the activity of the Cellic CTec2 enzyme mixture (Lot # SLBS6227) on filter paper. The protocol used was adapted from Xiao et al. and Adney et.al [36, 37]. The assay measured glucose by detecting the reducing sugars through a color reaction caused by di-nitrosalicylic acid. Samples were added to a Microtest Plate 96 Well,F plate and the absorption at 540 nm was measured using both a Spectro star nano BMG Labtech plate reader and a BMG FLUOstar OMEGA Microplate Reader after the color reaction. The activity was then calculated in terms of Filter Paper Units (FPU) per mL enzyme solution in accordance with the aforementioned protocols.

Hydrolysis method development

A method for conducting parallelized hydrolysis experiments under anaerobic conditions was developed. The system consisted of ten conical shake flasks containing the hydrolysate mixture inside a shake incubator with nitrogen gas bubbled through the hydrolysate. Tubing for gas was taped and zip-tied to the lab walls and ceiling. A needle valve and a manometer were added to the gas supply tubing to regulate and measure the gas flow. An Acro 50 w/ 0.2 nm PTFE membrane air filter ensured sterile nitrogen supply. Before reaching the shake flasks, the sterile nitrogen was bubbled through a Schott bottle filled with MilliQ water to moisturize the nitrogen and prevent excessive evaporation of the hydrolysate liquid during hydrolysis. The gas was spread to the shake flasks using a 1-to-10 branching tube made using Y-connectors.

To ensure similar flows in all tubes, water was first pumped through 1-to-5 branching tubes with the help of pressurized air. The relative volumes of water from each opening over a fixed amount of time were observed. Four manometers were then connected to separate ends of the branching tube with the fifth opening clamped. This was done because only four extra manometers were available. Using the Schott bottle and pressurized air, humidified air was passed through the system and the relative flow was noted. Measuring the humidified air flow rate was repeated until every opening on the branching tube had been clamped once. The four manometers were then removed. This allowed estimations to be made about the difference in flow rate between the different tubes.

A three-way-valve was added before the Schott bottle and the air filter to avoid nitrogen-enrichment in the shaker or in the room. Tubing was connected to the third opening leading off to a ventilation arm. Thereby, the nitrogen flowed directly to ventilation during sampling. Furthermore, the exhaust gas from the shake flasks was combined into one tube leading to the ventilation as well.

Three holes were drilled through each of ten rubber stoppers that had been temporarily solidified by liquid nitrogen: A larger center one and two smaller ones on either side of the larger hole. A 21cm long metal tube with an outer diameter of 6.05 mm and an inner diameter of 3.73 mm was tightly fitted through the center hole of each rubber stopper while two 10 cm

long metal tubes with an outer diameter of 3.3 mm and an inner diameter of 1.75 mm were tightly fitted through the smaller holes of each rubber stopper.

The system was tested to ensure that gas could pass through the slurry under realistic conditions. A 500 mL conical shake flask with 125g prepared slurry was made. The prepared slurry was made by adding 90.67 g of pretreated slurry from MAT.lB.108 so that the final WIS concentration would reach 10m%, 31.1 mL of 0.48 M NaOH to adjust the pH to 5.00 and 417 µL Cellic CTec 2 solution (VCSI0003) with a concentration of 150 FPU/mL to reach 5 FPU/g_{WIS} to the shake flask. MilliQ water was added to reach the final mass of 125 g. A rubber stopper was added and then connected to the system.

6.67 vvm of nitrogen gas was supplied to the shake flask and the shake incubator was set to 30 °C and 180 rpm for 3 hours. As sampling from the central metal tube was impossible under realistic conditions due to the high heterogeneity of the slurry, the system was changed to serve gas only. Sampling was performed manually from the shake flask by lifting the stopper. The shaking speed was set to 120 rpm.

The method was refined during the hydrolysis experiments. The gas flow was lowered from 6.67 vvm to 3.33 vvm during the second set of hydrolysis experiments. The combinatory setup between the branching tube, each shake flask and the debranching tube went through a couple of revisions. Tubes and branches were labelled from the second experiment on and arranged as shown in Table 6 and Figure 2. A schematic overview of the system can be seen in Figure 3.

Table 6 – Arrangement description of the connections for the branching tubes (a-j) with the shake flasks (1-10) and the debranching tubes (A-J) for the second to fourth set of hydrolysis experiments.

Set 2	Set 3	Set 4
a1A	a3A	a5A
b2B	b5B	b6B
c3C	c6C	c4C
d4D	d8D	d7D
e5E	e1E	e3E
f6F	f4F	f8F
g7G	g7G	g1G
h8H	h10H	h2H
i9I	i2I	i9I
j10J	j9J	J10J

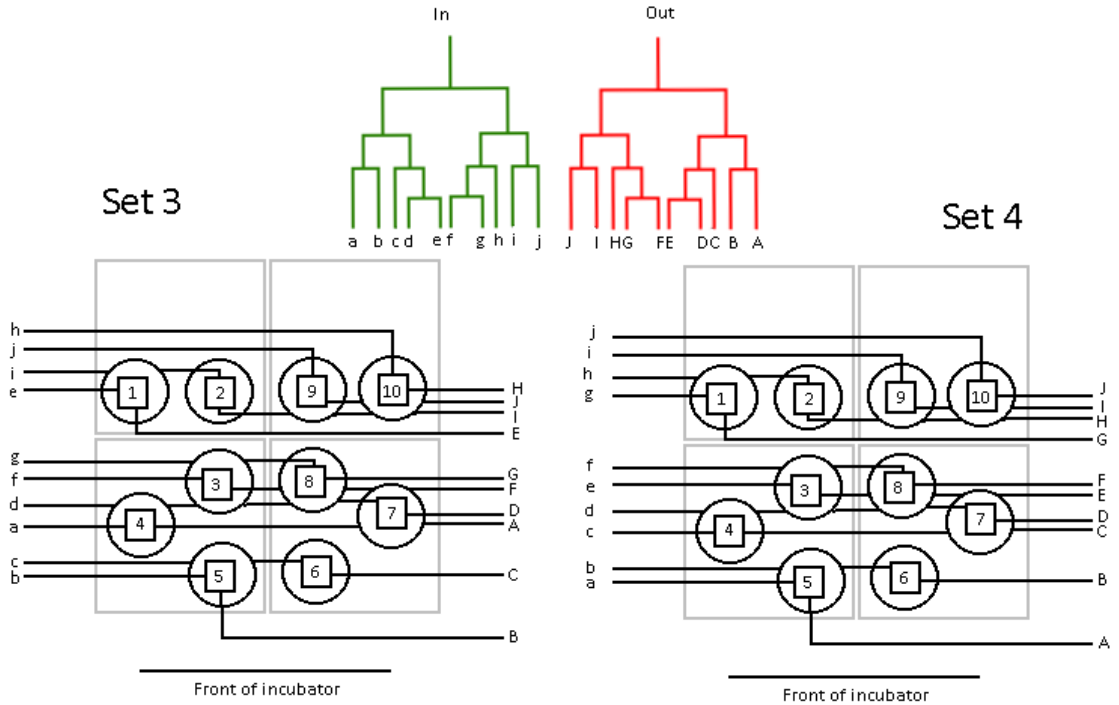

Figure 2 – Connections of the branching tubes (a-j) with the shake flasks (1-10) and the debranching tubes (A-J) for the third and fourth set of hydrolysis experiments seen from above. The green tree diagram depicts the branching tube while the red tree diagram depicts the debranching tube. "In" denotes where the gas inlet to the incubator and "Out" denotes the outlet of the gas flows from the incubator. Circles symbolize the shake flasks, squares the stoppers, gray squares in the background the four sticky pads in the incubator and the remaining lines tubing. The numbers represent the flask ID and sampling order.

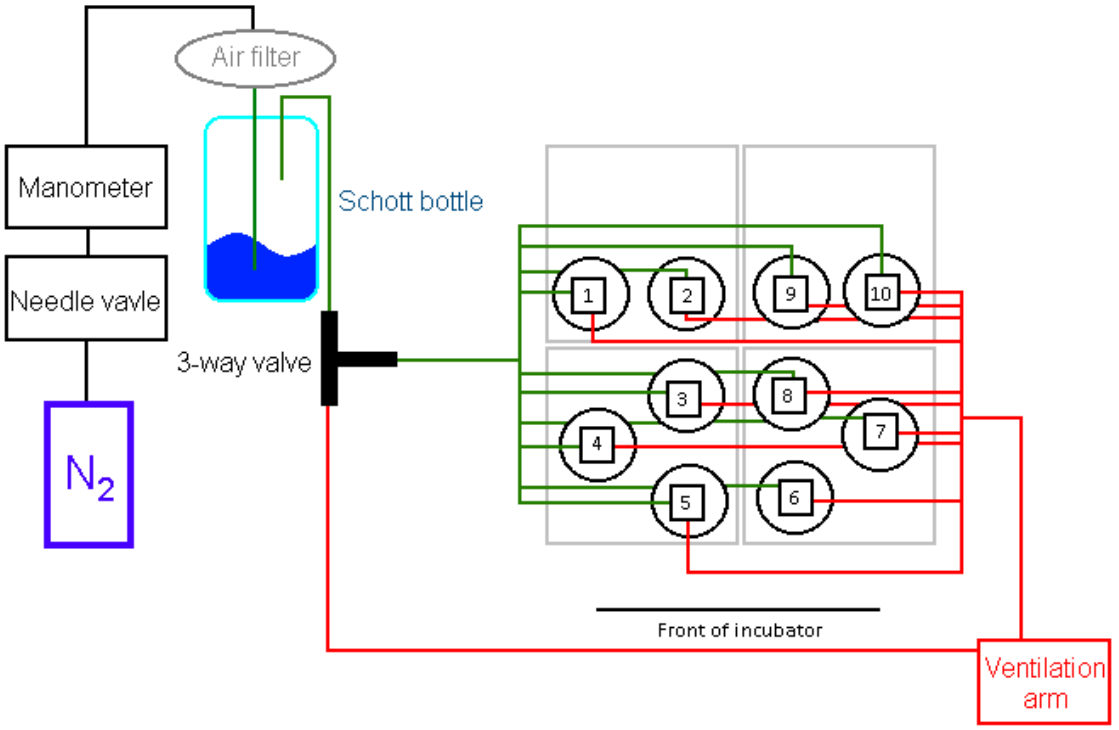

Figure 3 – Schematic overview of the hydrolysis experimental setup. Nitrogen gas travelled from the wall through the needle valve, manometer and air filter into the water-filled Schott bottle where it got moisturized. The gas then travelled either into the incubator and shake flasks following the green path or directly to the ventilation arm following the red path, depending on the setting of the 3-way valve. The ventilation arm also vented the gas from the shake flasks.

Hydrolysis of spruce residues

Four sets of hydrolysis experiments were carried out in shake flasks at 30 °C under sparging with nitrogen gas through the hydrolysate and a mixing speed of 120 rpm for 72 h. Sampling was conducted at 0, 3, 6, 9, 24, 25, 26, 33, 48 57, and 72 h after hydrolysis start. The hydrolysis experiments were carried out using the pretreated slurry of material MAT.lB.107 as it was one of the center points in the experimental design of the pretreatment. After the hydrolysis the hydrolysate was tested for microbial contamination by plating 100 µL of hydrolysate diluted 1:10 in sterile MilliQ water on yeast peptone dextrose (YPD) agar plates. The plates were incubated for 48 hours at 35 °C in a shaking incubator and colony forming units were counted. 10 grams of hydrolysate from each control sample after 72 hours of hydrolysis was used for WIS determination. After washing the hydrolysate, the collected supernatant with trace amounts of WIS was then consecutively centrifuged and the supernatant was discarded to estimate the error of the WIS measurement.

Hydrolysis experiments

The total weight of each experiment was 125 g. The experiments contained 10m% of WIS, they had an enzymatic activity of 8.5 FPU/g_{WIS} and a citrate buffer concentration of 43.16 mmol/g at an initial pH of 5.0. The remainder was MilliQ water sterilized by autoclavation and inhibitor. Six control experiments were conducted without the addition of any inhibitor. The influence of ten potential inhibitors were tested in duplicates: Glycerol (10 g/L), formic acid (1 g/L), HMF (2 g/L), furfural (0.83 g/L), levulinic acid (2 g/L), ethanol (70 g/L), acetate (1.6 g/L), glucose (20 g/L), xylose (5 g/L) and a mixture of arabinose, rhamnose, galactose and mannose (ARGM) (in total 12.5 g/L). The ARGM solution was split 10.28m%, 6.86m%, 24.49m% and 58.37m% between arabinose, rhamnose, galactose and mannose respectively. These percentages were calculated from the characterization of the material to be near identical to the slurry. The inhibitor concentrations listed above indicate the target initial concentration in the liquid fraction of the hydrolysate.

For HMF, furfural, levulinic acid, acetate and formic acid; the above mentioned concentrations were derived by taking the difference between the concentrations of inhibitors in MAT.lB.107 in the liquid fraction and the concentrations of inhibitors in the batch of pretreated slurry with the highest concentration of the specific inhibitor in the liquid fraction. These values were then increased by 10-15% depending on the compound, to account for uncertainties in the composition measurements. For the sugars, the concentration increase was derived by calculating the theoretical maximum amount of releasable sugar monomers and the concentration was then increased by 5%. The concentration increase of ethanol was set due to the project requirement that the finished process, including both hydrolysis and fermentation must work under ethanol concentrations of 70 g/L.

Sampling was conducted by removing 3-4 mL of slurry using 5 mL serological pipettes with cut tips. The sample was weighed in 15 mL falcon tubes and centrifuged at 5000 rpm at 4 °C for 12 min. The liquid fraction was filtered through 25 mm w/ 0.2 µm PTFE membrane syringe filters. The solid and liquid fractions were then frozen at -20 °C until analysis. The

liquid fraction was analyzed using the HPLC and samples were diluted 1:3. Calibration curves derived during characterization was used to integrate the peaks and obtain the concentration of each hydrolysis sample.

Remainders from each hydrolysis set were collected and frozen at -20 °C. From the first and second set, 10 g from each sample was collected and stored, and from the remaining sets, all remaining slurry was collected and stored.

For deriving the glucose produced and the productivity the three assumptions below were made. The third assumption was made because time restrictions prohibited the measurement of the WIS for every sample and without that parameter the glucose production and productivity for the hydrolysis could not be calculated (See Table 7).

1. Each sample taken from the shake flask is representative of the entire flask.
2. The density of the liquid fraction does not change during the hydrolysis.
3. The WIS remains at 10m% throughout the hydrolysis.

To calculate the amount of glucose produced during each of the sampling times nine quantities were used which are listed in Table 7.

Table 7 – List of quantities used to calculate the mass of glucose produced during hydrolysis. *WIS* denotes the percentage of water insoluble solids and is assumed to be equal to 0.1. ρ_{liq} is the density of the liquid fraction and is assumed to be constant. *i* denotes the i'th sample in chronological order of any one specific hydrolysis experiment.

Quantity	Initial value (i = 0)	Sequential value (1 ≤ i ≤ 10)	Description
C_{glc}	According to data	According to data	Concentration of glucose in the liquid fraction at each sampling. (g L^{-1})
m_{tot}	125g	$m_{tot,i-1} - m_{rem,i-1}$	Mass of slurry in the shake flask prior to sampling. (g)
m_{rem}	According to data	According to data	Mass of slurry removed during each sampling. (g)
mg L_c	$C_{glc,0} * \frac{m_{tot,0} * (1 - WIS)}{\rho_{liq}}$	$C_{glc,i} * \frac{m_{tot,i} * (1 - WIS)}{\rho_{liq}}$	Mass of glucose in the shake flask prior to sampling. (g)
mg $L_{c,rem}$	$m_{rem,0}/m_{tot,0} * m_{glc,0}$	$m_{rem,i}/m_{tot,i} * m_{glc,i}$	Mass of glucose removed during each sampling. (g)
mg $L_{c,prod}$	0g	$m_{glc,i} - m_{glc,0} + \sum_{n=1}^{i-1} m_{glc,rem,n}$	Mass of glucose produced after each sampling. (g)

Productivity expressed as mass glucose produced per hour and mass WIS was calculated using equation 2.

$$P_{t_j,t_i,t_k} = \frac{1}{WIS}\left(\left(\frac{t_j - t_i}{t_k - t_i}\right)\frac{m_{glc,prod,k} - m_{glc,prod,j}}{t_k - t_j} + \frac{m_{glc,prod,j} - m_{glc,prod,i}}{t_j - t_i}\left(\frac{t_k - t_j}{t_k - t_i}\right)\right) \quad (2)$$

P_{t_j,t_i,t_k} is the estimated productivity in the jth time point using the ith and kth time point where $i<j<k$. t_a is the time since hydrolysis start for time point a.

For each of the ten hydrolysis experiments and the controls, the estimated glucose productivity $P_{6,3,9}$ and $P_{26,24,33}$ was calculated. A regression line was fitted and its slope, hence the estimated average increase in productivity per hour of each experiment between time point 6 and 26 was calculated.

The maximal productivity between three consecutive time points was also calculated for each pair of hydrolysis experiment duplicates using the following formula:

$$P_{max} = \max\left(P_{t_j,t_{j-1},t_{j+1}}\right), 2 \leq i \leq 10, i \in \mathbb{N} \quad (3)$$

Four different average yields were also calculated. The yields were mass glucose produced per mass cellulose present at hydrolysis start, mass glucose produced per mass WIS present at

hydrolysis start, mass glucose produced per mass slurry present at hydrolysis start, and theoretical yield, i.e. mass glucose produced per maximal theoretical mass of glucose released. All yields are linearly proportional to each other and the total mass of glucose produced. Their respective formulas are presented below in equation 4-7.

$$Y_{Glc/_{cell}} = \frac{1}{n}\sum_n \frac{m_{glc,prod,10,n}}{m_{tot,0} * WIS * f_{cell}} \quad (4)$$

$$Y_{Glc/_{WIS}} = \frac{1}{n}\sum_n \frac{m_{glc,prod,10,n}}{m_{tot,0} * WIS} \quad (5)$$

$$Y_{Glc/_{Slurry}} = \frac{1}{n}\sum_n \frac{m_{glc,prod,10,n}}{m_{tot,0}} \quad (6)$$

$$Y_{Glc/_{glc_{max}}} = \frac{1}{n}\sum_n \frac{m_{glc,prod,10,n}}{m_{glc,max}} \quad (7)$$

n in equation 4-7 denotes the number or replicates for each hydrolysis experiment. *WIS* equals 0.1 g/g in equation 4-5 and f_{cell} in equation 4 represents the mass fraction of cellulose in the dried, pretreated material. $m_{glc,max}$ in equation 7 represents the maximal mass of releasable sugars which is derived by multiplying the mass fraction of polymeric glucose per gram pretreated slurry with the mass of pretreated slurry used in any hydrolysis experiment.

A Mann–Whitney U test was performed on the yields to compare the medians of the control samples compared to each of the samples with added inhibitors. Significance levels used were 5% and 10%.

Results

In this section the results from the experiments described in the method section are presented. For HPLC results derived from the HPLC with both UV/VIS and RI detection, only the RI data will be presented, as it was evident that data from the RI-spectra were more reliable than the data from the UV/VIS spectra.

Method development of hydrolysis experiments

The system developed can process ten 72 h hydrolysis experiment per working week, including preparation and cleaning of the system. Sampling, separation of the samples into liquid and solid fraction, and filtration of the liquid fraction take 40-60 min. The system is durable and can be reused many times. The only parts which need replacement are zip-ties between tubing joints. The system is safe to operate and not prone to failing. Parallelization is possible and gas can be supplied to several shake flask reactors simultaneously and with similar flow, albeit not equally. The relative standard deviation for the mass of glucose produced from the 6 control samples was 6.4%, which indicates reliability of the system.

Sampling through the central tube was not possible due to the heterogeneity of the slurry which clogged the central tube.

Method development of HPLC columns

Table 8 shows the retention time in the isocratic HPLC using the Rezex ROA column for each compound investigated. For column, program and systems details, see the section "Analysis methods". Trans-ferulic acid and ferulic acid were the only compounds investigated that could not be identified. All compounds except HMF, furfural and vanillin eluted before 20 minutes.

Table 8 – Retention time, in minutes, for all the single standards tested in the HPLC. Galactose, mannose and xylose co-elute in both the UV/VIS spectrum and in the RI-spectrum.

Substance	Peak UV/VIS	Peak RI
Citrate	6.63	6.71
Glucose	no peak	7.47
Xylose	7.83	7.97
Mannose	7.83	7.92
Galactose	7.875	7.96
Glycerol	no peak	10.7
Formic acid	no peak	10.91
Acetate	11.88	11.97
Levulinic acid	13.05	13.14
Ethanol	no peak	16.44
HMF	25.37	25.46
Furfural	36.98	37.08
Vanillin	no peak	93
Ferulic acid	not found	not found
Trans-ferulic acid	not found	not found

The remainder of this subsection will present the results from the HPLC column method development for the hydrolysate experiments.

Kinetex F5 column

Testing different fractions of water and ACN as the mobile phase showed that higher fraction of water led to prolonged elution times while lower fraction of water led to co-elution of the peak and poor baseline separation. Testing different detection wavelengths with the PDA-detector resulted in minute differences on the span 210 nm – 240 nm for the detection of HMF and furfural. Investigating the differences between using 0.1v% H_3PO_4 or water in the mobile phase failed to demonstrate any appreciative difference. Peaks for furfural, HMF and sorbic acid could be identified while peaks for organic acids could not. Several unknown peaks were also observed. The chromatograms can be view in Figure 4.

Figure 5 compares differences between running isocratically using 80% MilliQ water and 20% ACN as the mobile phase and with a sharp gradient that changed the fraction of ACN from 5% to 20% 2 minutes after injection. The sharp gradient gave the chromatogram a clear baseline as compared to Figure 4. It also extended the elution time for the compounds tested compared with an isocratic method.

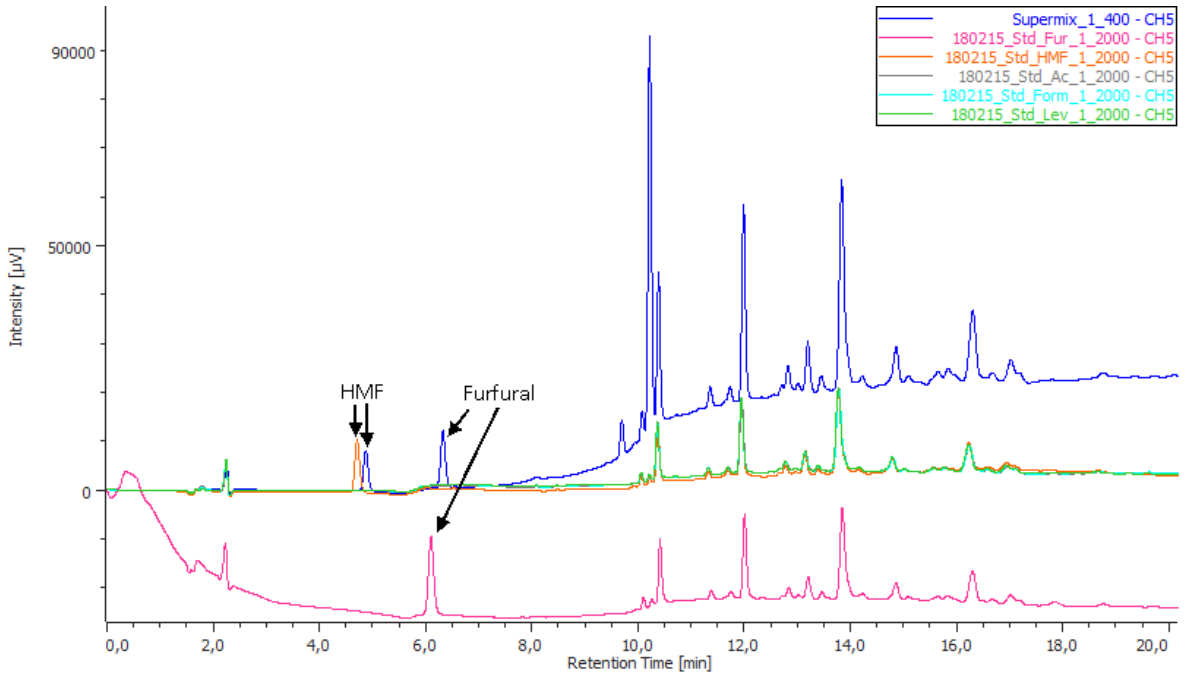

Figure 4 – Results from running furfural (5 mg L^{-1}), HMF (5 mg L^{-1}), vanillin (1.25 mg L^{-1}), acetate (6.25 mg L^{-1}), citrate (7.5 mg L^{-1}), formic acid (2.5 mg L^{-1}), levulinic acid (1.25 mg L^{-1}), and sorbic acid (3.75 mg L^{-1}) (blue curve) with 0.1v% H_3PO_4 and ACN as the mobile phase compared to furfural (5 mg L^{-1}) (pink curve), HMF (5 mg L^{-1}) (orange curve), acetate (6.25 mg L^{-1}) (gray curve), formic acid (2.5 mg L^{-1}) (cyan curve) and levulinic acid (1.25 mg L^{-1}) (green curve) with MilliQ water and ACN as the mobile phase on the Kinetex F5 column. Peaks not labeled are unidentified. The dead time peak can be seen soon after the 2 min mark in all chromatograms.

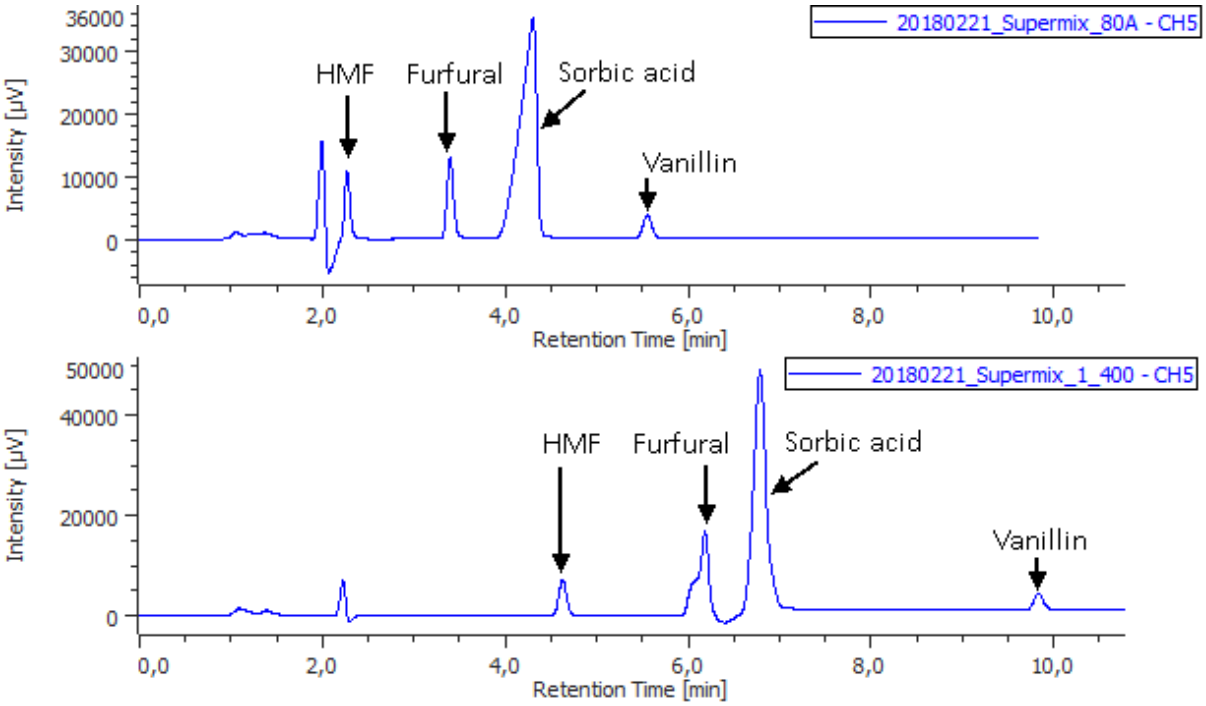

Figure 5 – Results from running furfural (5 mg L^{-1}), HMF (5 mg L^{-1}), vanillin (1.25 mg L^{-1}), and sorbic acid (3.75 mg L^{-1}) on the Kinetex F5 column. Top: compounds run isocratically with 80% MilliQ water and 20% ACN as the mobile phase on the Kinetex F5 column. Bottom: 2 min with 95% MilliQ water and 5% ACN then 8 minutes with 80% MilliQ water and 20% ACN. The dead time peak can be seen soon after the 2 min mark in all chromatograms.

Calibration curves for HMF and furfural when using the Kinetex F5 column are listed in Table 9 together with calibration curves for HMF and furfural when using the Rezex ROA column on the isocratic HPLC which was the setup used during initial characterization of the material. The slope of the calibration curves were 315 times higher for the Kinetex F5 column compared to the Rezex ROA column. The chromatograms of the calibrations series for HMF and furfural with the Kinetex F5 column are described in Figure 6. The detection limit was 2.9 magnitudes lower with the Kinetex F5 column compared to the Rexez ROA column.

Table 9 - The line parameters for the calibration curves of HMF and furfural developed on the gradient HPLC using the Kinetex F5 column and the calibration curves of HMF and furfural developed on the isocratic HPLC using the Rezex ROA column. Detection range for the Kinetex F5 column was 200 µg L^{-1} – 200,000 µg L^{-1} while the detection range for the Rezex ROA column was 160 mg L^{-1} – 10,000 mg L^{-1}.

Compound	Column	Slope [µVL/g]	Intercept [µV]	R^2
HMF	Kinetex F5	23818900	-33123.1	0.99256
Furfural	Kinetex F5	19323300	17875.7	0.999631
HMF	Rezex ROA	66818.2	1029.05	0.999986
Furfural	Rezex ROA	64503.3	1490.53	0.999992

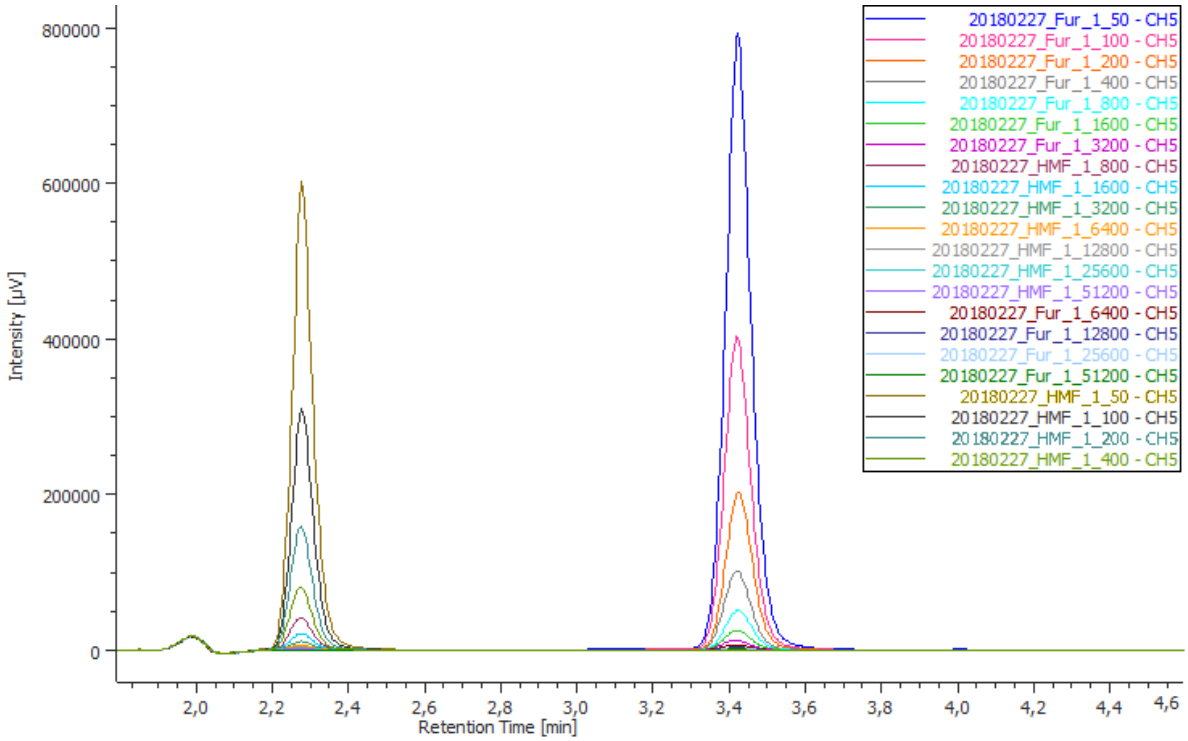

Figure 6 – Results showing HMF calibration series (2.2-2.4 min) and furfural calibration series (3.3-3.6 min) on the Kinetex F5 column. Highest concentration for both compounds is 200 mg L^{-1} and each consecutive dilution is twice as diluted as the previous down to a final concentration of 195 µg L^{-1}. The dead time peak can be seen around 2 min.

Rezex Pb column

Method development on the Rezex Pb column never yielded a method that was able to get proper base line separation. Severe co-elution was consistently a problem. No quantitative method was developed.

Figure 7 and Figure 8 shows the results from differing the flow rate and temperature, respectively. This was done to try to improve the separation of the peaks. Higher temperatures caused ethanol to elute faster. Higher flow and higher temperature rate lead to improved peak separation. The mobile phase in Figure 7 was MilliQ water while in Figure 8 the mobile phase was 0.4v% methanol.

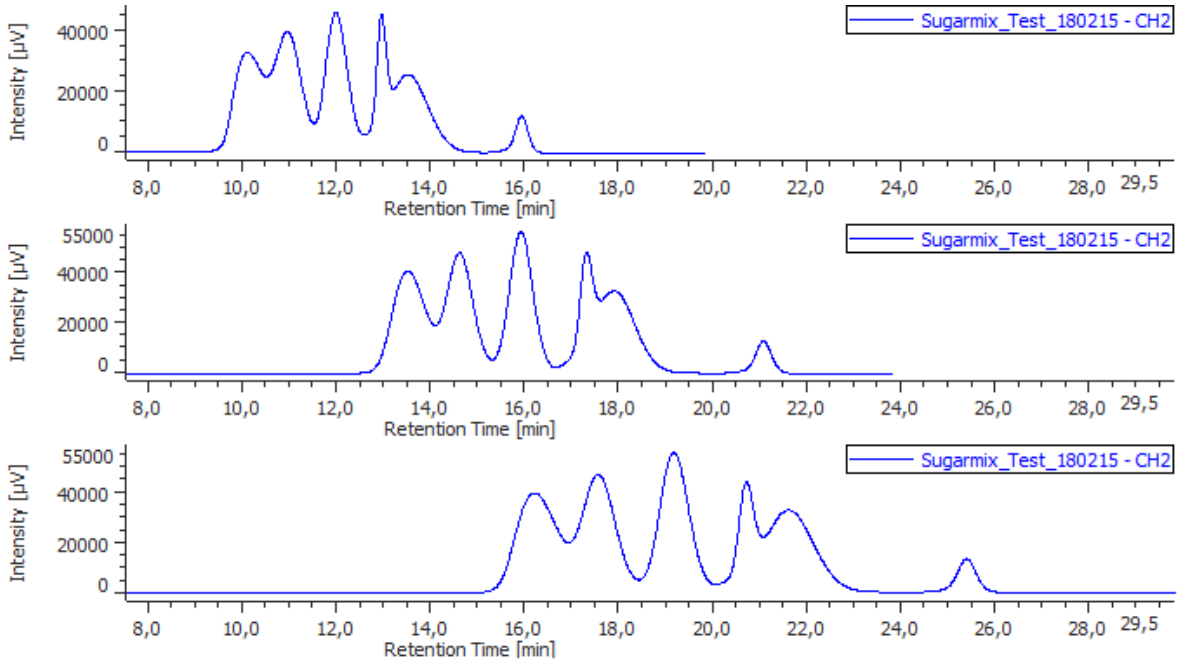

Figure 7 – Results from running glucose (25 g L^{-1}), xylose (25 g L^{-1}), galactose (25 g L^{-1}), ethanol (25 g L^{-1}), mannose (25 g L^{-1}), and glycerol (5 g L^{-1}) (blue curves) on the Rezex Pb column, eluting respectively with different mobile phase speeds. Top: 0.5mLmin^{-1}. Middle: 0.6mLmin^{-1}. Bottom: 0.8 mL min^{-1}. The temperature was 80 °C.

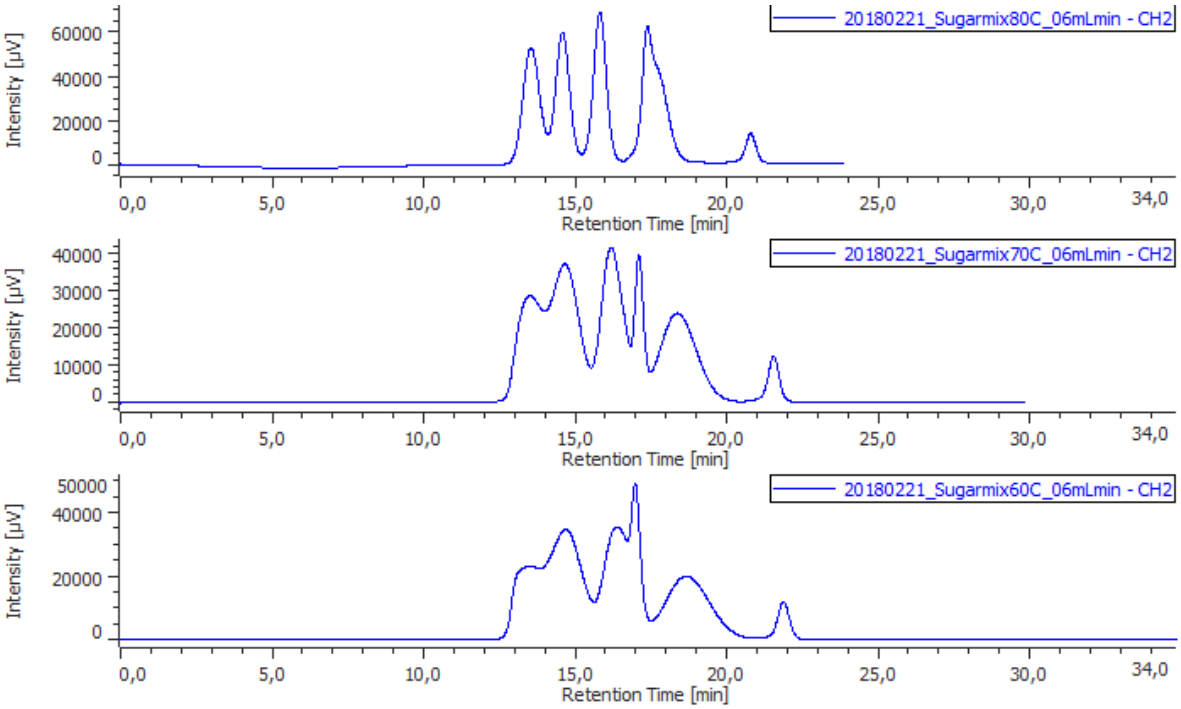

Figure 8 – Results from running glucose (25 g L^{-1}), xylose (25 g L^{-1}), galactose (25 g L^{-1}), ethanol (25 g L^{-1}), mannose (25 g L^{-1}), and glycerol (5 g L^{-1}) (blue curves) on the Rezex Pb column, eluting respectively with different temperatures. Top: 80 °C, middle: 70 °C, bottom: 60 °C. The flow rate was 0.6 mL min^{-1}.

Figure 9 shows an identification of the different peaks for the sugars and alcohols of interest. Glucose, xylose, rhamnose, and galactose co-eluted with each other as well as ethanol, arabinose and mannose. Figure 10 shows an identification of the different peaks in a

hydrolysate control sample. With representative concentration rations between the analytes, the peak separation was even worse.

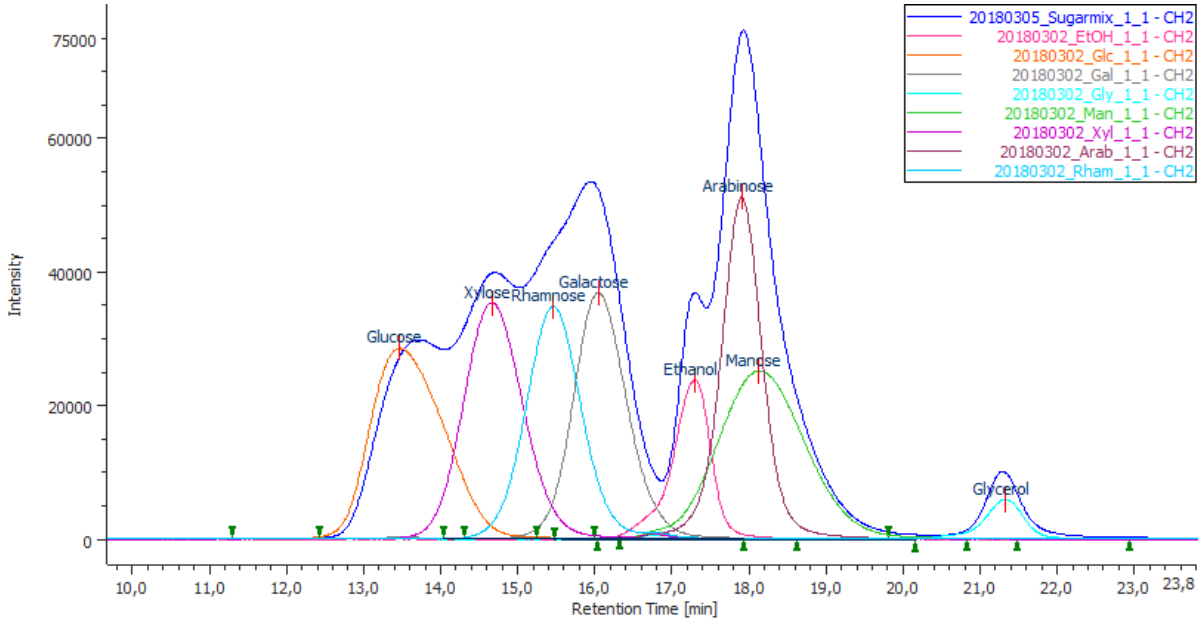

Figure 9 – Results from running glucose (25 g L^{-1}), xylose (25 g L^{-1}), rhamnose (25 g L^{-1}), galactose (25 g L^{-1}), ethanol (25 g L^{-1}), arabinose (25 g L^{-1}), mannose (25 g L^{-1}), and glycerol (5 g L^{-1}) on the Rezex Pb column, eluting respectively, both as a combined standard (dark blue curve) and as single standards (remaining curves). The temperature was 80 °C, flowrate 0.6 mL min^{-1} with milliQ water as eluent.

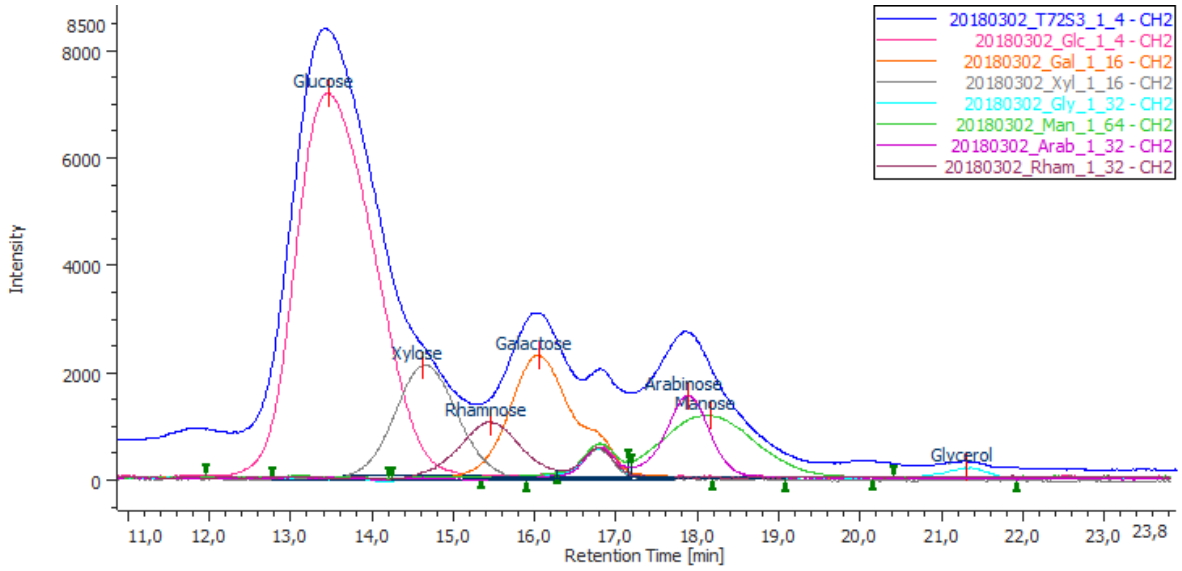

Figure 10 – Results from running control sample #4 after 72 hours of hydrolysis (blue curve) against single standards with representative concentrations (remaining lines) on the Rezex Pb column: Glucose (6.25 g L^{-1}), xylose (1.563 g L^{-1}), rhamnose (0.7813 g L^{-1}), galactose (1.563 g L^{-1}), arabinose (0.7813 g L^{-1}), mannose (0.3906 g L^{-1}), and glycerol (0.1563 g L^{-1}). The temperature was 80 °C, flowrate 0.6 mL min^{-1} with milliQ water as eluent.

Rezex ROA column

The Rezex ROA column provided very similar result on the gradient HPLC as previously observed during characterization on the isocratic HPLC. The main difference was the inability to detect sugars or alcohols, i.e. glucose, galactose, mannose, xylose, ethanol, and glycerol, due to the use of the photo diode detector. Citrate caused two peaks instead of one as when analyzing with RI instead of PDA. In Figure 11 all the peaks identified are shown. The retention times were very similar to the ones listed in Table 8.

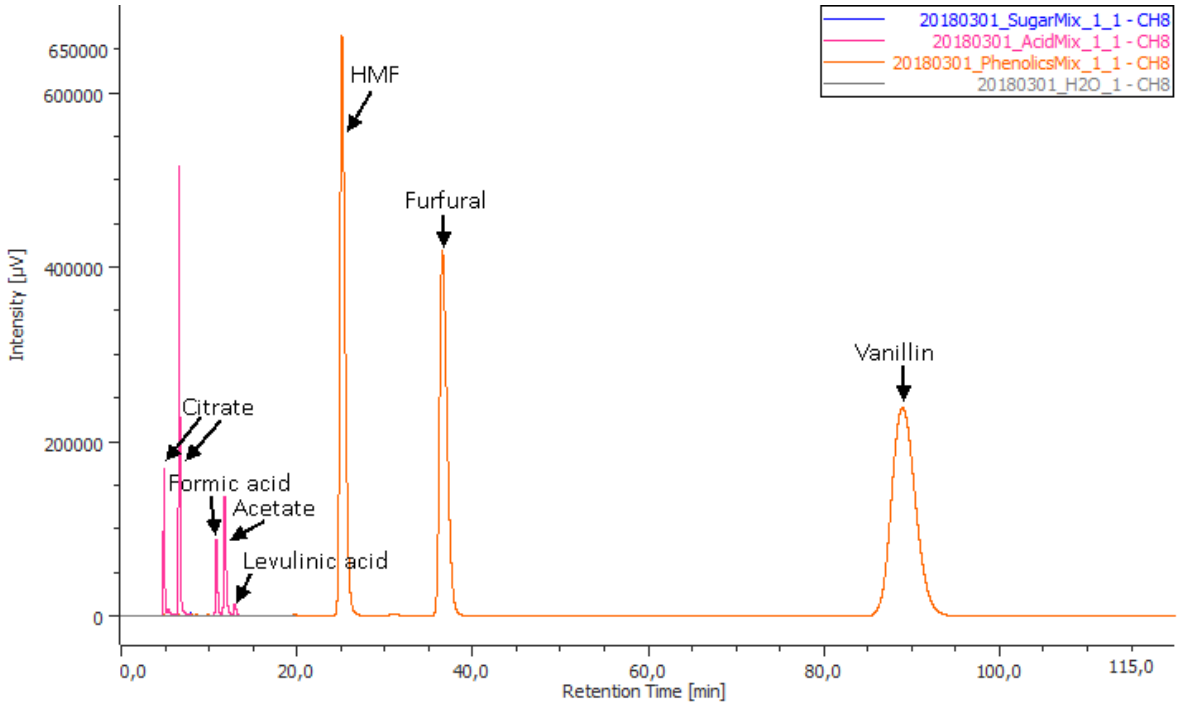

Figure 11 – Results from running glucose (25 g L^{-1}), galactose (25 g L^{-1}), mannose (25 g L^{-1}), xylose (25 g L^{-1}), ethanol (25 g L^{-1}), glycerol (5 g L^{-1}), HMF (10 gL^{-1}), furfural (10 g L^{-1}), levulinic acid (2.5 g L^{-1}), acetate (12.5 g L^{-1}), citrate (15 g L^{-1}), and formic acid (5 g L^{-1}) on the Rezex ROA column. Acids (pink curve) were all identified as well as the aromatics (orange curve). The sugars and alcohols (blue curve) could not be detected. The temperature was 80°C, the flowrate 0.8 mL min^{-1} and the eluent was 5 mM H_2SO_4.

Composition of pretreated spruce residue slurry

In the figures and tables below the averages of the replicates for each pretreated materials are presented. The ID for each pretreatment has been shortened for convenience. For example; MAT.lB.104 are presented as '104' in the diagrams below. For pretreatment condition details, see Table 4.

In Figure 12 and Figure 13 the average total glucose and hemicellulose sugars for each fraction are presented in order of increasing severity factor. MAT.lB.104-105 and MAT.lB.106-109, which each had the same pretreatment conditions showed similar results. The pretreatment used on MAT.lB.110 yielded the highest percentage of releasable sugars for both cellulose and hemicellulose sugars. The percentage of releasable sugars for MAT.lB.110 was 13.0m% with a severity factor of 4.07. The percentage of releasable sugars decreased with increasing severity factor over 4.07.

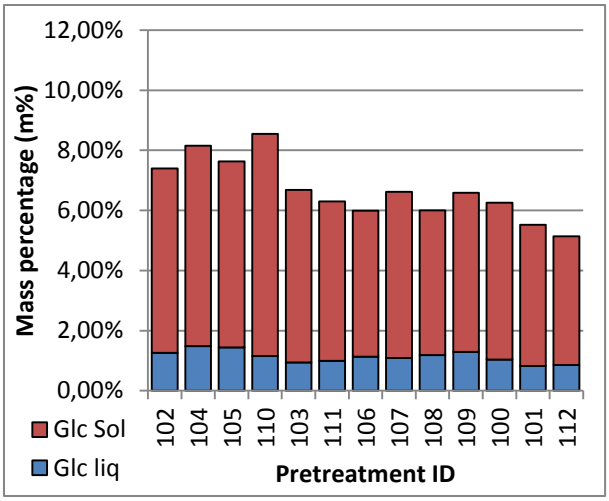

Figure 12 – The average mass percentage (m%) of releasable glucose (Glc) in pretreated slurry from each of the fractions for each of the pretreatments sorted by increasing severity factor. Red (top) is the percentage of releasable glucose from the solid (sol) fraction. Blue (bottom) is the percentage of releasable glucose from the liquid (liq) fraction.

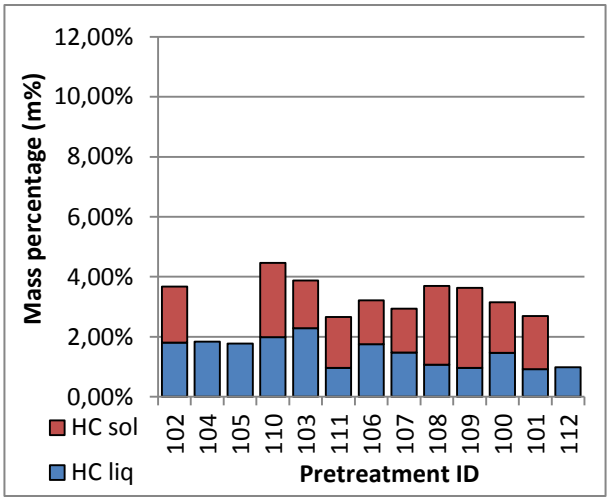

Figure 13 – The average mass percentage (m%) of releasable hemicellulose (HC) sugars, i.e. xylose, mannose, galactose & arabinose, in pretreated slurry from each of the fractions for each of the pretreatments. Red (top) shows the percentage of hemicellulose sugars from the solid (sol) fraction. Blue (bottom) shows the percentage of hemicellulose sugars from the liquid (liq) fraction. Rhamnose is not included because it did not reach the limit of quantification during analysis.

Liquid fraction

The density of the liquid fraction of the pretreated slurry from MAT.lB.109 was measured to estimate potential significant errors in sample preparation during the hydrolysis experiments. It was measured with two replicates to 1.0463 g L^{-1} and 1.0395 g L^{-1} with an average density of 1.0429 g L^{-1} and a relative standard deviation of 0.4602%.

Figure 14 depicts the concentration of alcohols, organic acids, and aromatics in the liquid fraction as calculated with the RI data from the HPLC in order of increasing severity factor for each of the pretreated materials. Lowest concentrations of the measured compounds were found in material MAT.lB.103. Figure 15 depicts the concentration of sugars in the liquid fraction as calculated from the IC in order of increasing severity factor. No clear trends can be observed in this figure. Figure 16 presents the average concentration for all quantifiable compounds over all pretreatments. Apart from glucose being the dominant compound measured, acetate and HMF are shown to be present at similar concentrations as each of the hemicellulose sugars.

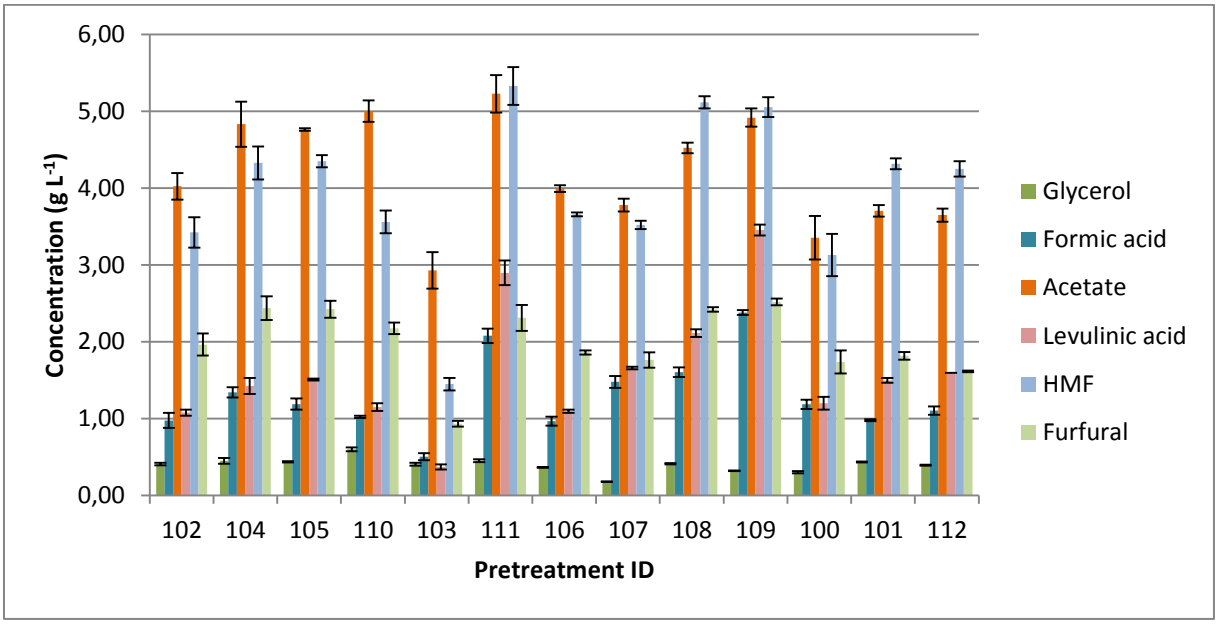

Figure 14 – Average concentrations of alcohols, acids and aromatics for each pretreatment in the liquid fraction. Citrate, ethanol and vanillin are not shown because the amounts were either not existent, below the detection limit or below the quantification limit. Error bars shows 1 standard deviation in each direction from the mean (n=2-3).

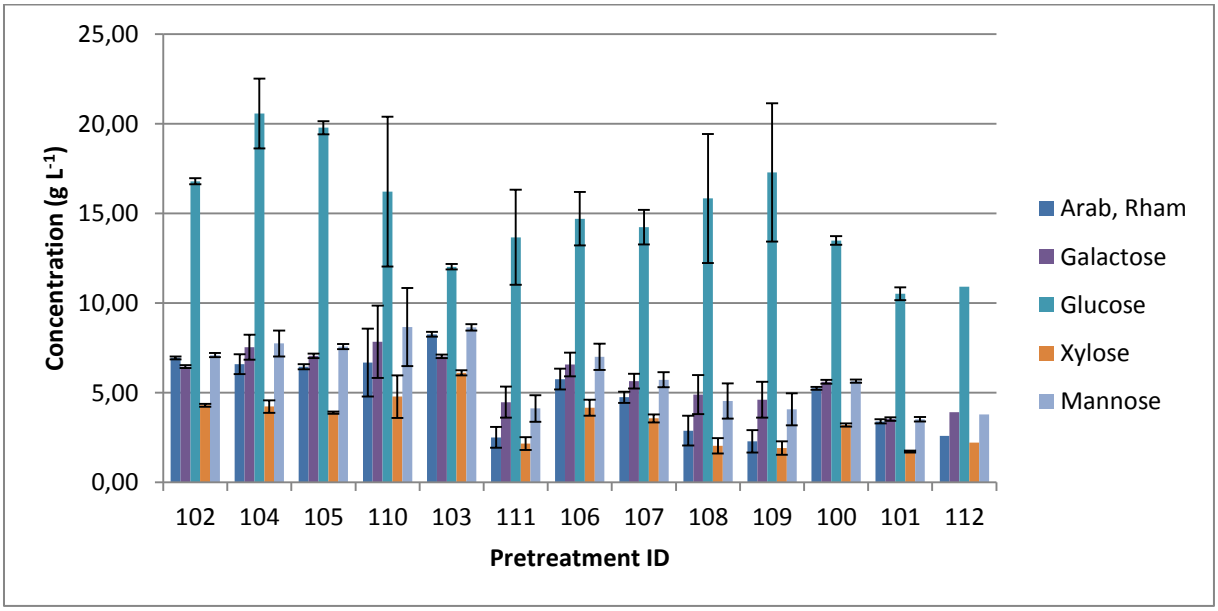

Figure 15 - Average concentrations of sugars of the triplicates for each pretreatment in the liquid fraction. Arabinose and rhamnose (Arab, Rham) are represented as one item due to co-elution of the peaks. Pretreatment 112 was only analyzed as a singlet. Error bars shows 1 standard deviation in each direction from the mean (n=3).

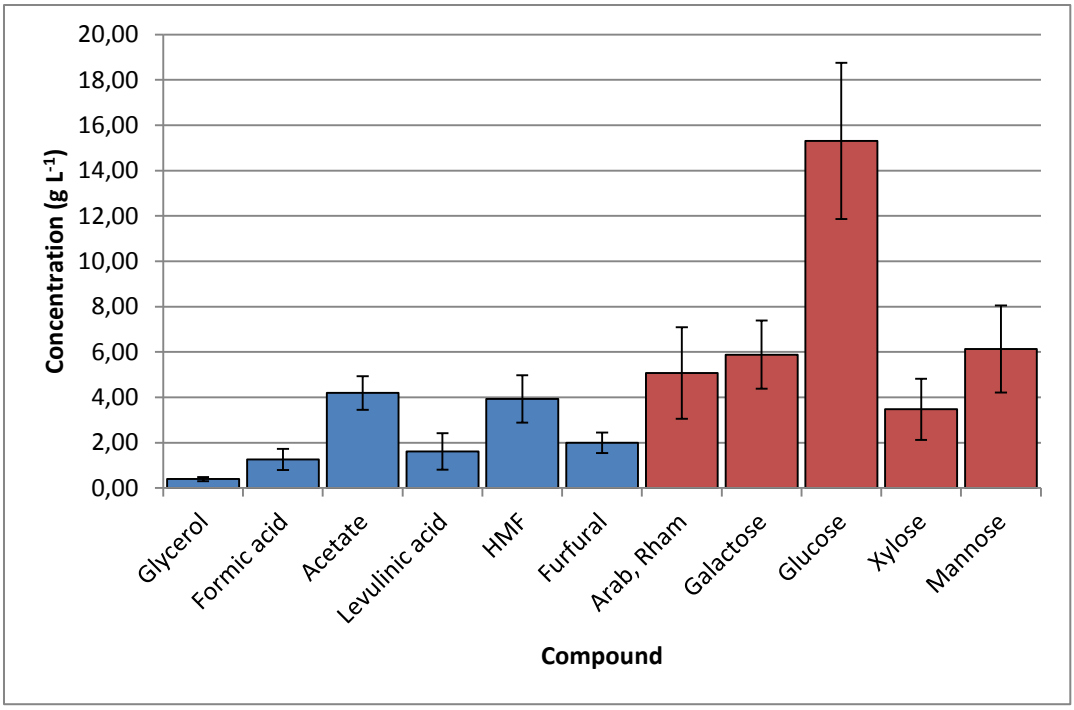

Figure 15 – Average concentration of all pretreatments for each compound in the liquid fraction. Blue bars show the results from HPLC analysis while red bars show the result from IC analysis. Arabinose and rhamnose (Arab, Rham) are represented as one item due to co-elution of the peaks. Citrate, ethanol, and vanillin are not shown because the amounts were below the quantification limit. Error bars shows 1 standard deviation in each direction from the mean (n=37) .

Solid fraction

Figure 17 and Figure 18 present the results for the polymeric sugar content of the solid fraction for each the pretreatment materials in order of increasing severity fraction. The recovery rates used in equation 1 for which the results of Figure 17 and Figure 18 are dependent on can be found in Table 16 in the appendix. No clear trend could be seen for cellulose in Figure 17. Xylan and arabinan were lowest for an intermediary severity factor of 4.34 while galactose and mannose showed the highest concentration for an intermediary severity factor.

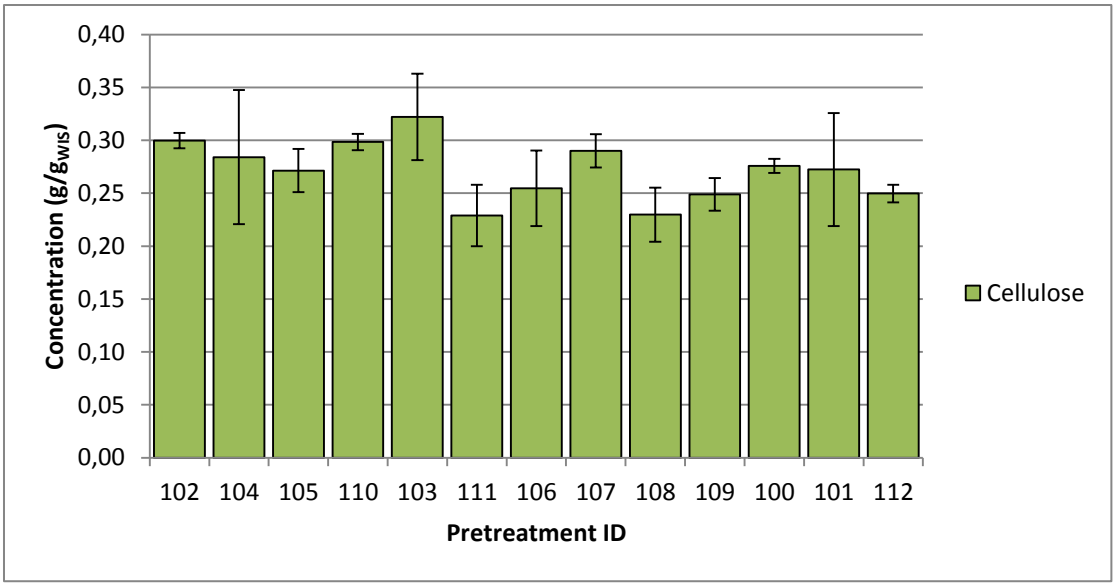

Figure 16 – Average concentration of cellulose in g/g_{WIS} of the triplicates for each pretreatment in the solid fraction. Material MAT.lB.104, MAT.lB.105 and MAT.lB.108 were made in hexaplicates. Error bars shows 1 standard deviation in each direction from the mean (n=3-6).

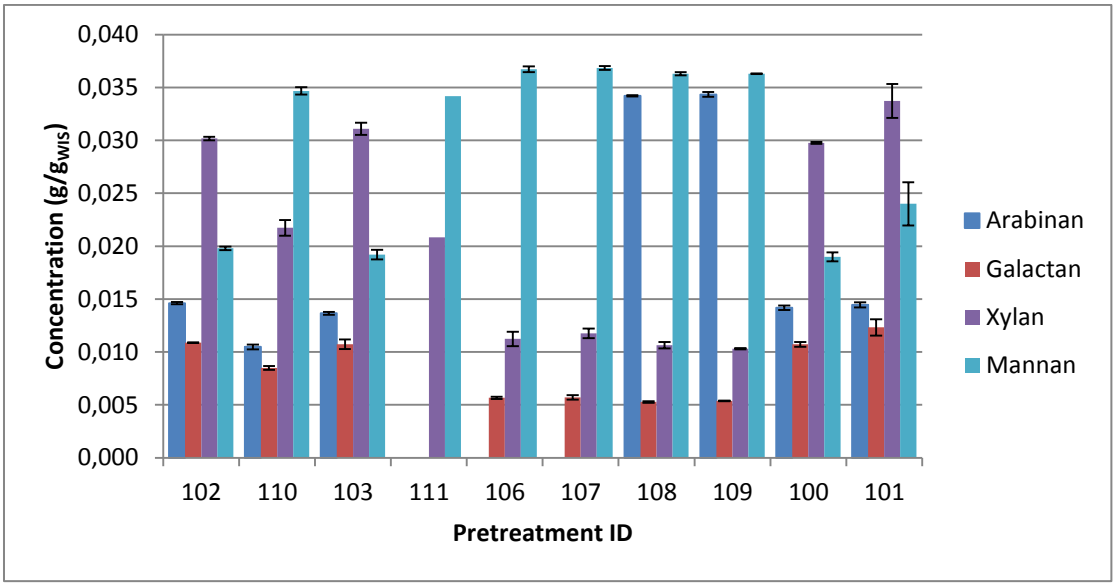

Figure 17 - Average concentrations of hemicelluloses in g/g_{WIS} of the triplicates for each pretreatment in the solid fraction. Material MAT.lB.108 was made in hexaplicates. Data for MAT.lB.104-105, Mat.lB.111 and rhamnan concentrations are not shown because the concentration of sugars was below the quantification limit. Error bars shows 1 standard deviation in each direction from the mean (n=3-6).

Hydrolysis result

Composition results for each hydrolysis are not shown in this section but instead the control samples will be used as an example and deviations from this will be commented on. Glycerol concentrations were consistently below the quantification limit and have thus been omitted. Productivity and yields are presented based on glucose produced from all hydrolysis experiments.

WIS content in hydrolysate

The WIS content was determined for the control samples after 72 hours of hydrolysis (Table 10). Some variance between the samples was observed and while the average WIS increased when taking the leftover solids from the washing into account, the relative standard deviation decreased.

Table 10 – WIS content expressed in terms of grams WIS per gram slurry (g/g) of the hydrolysate after 72h of hydrolysis for the six controls. The error adjusted (adj.) WIS (see p. 18) takes into account the solids that were left in the supernatant after washing while the non-error adjusted WIS does not.

Sample name	Error adj. WIS (g/g)	Non-error adj. WIS (g/g)
Control sample 1	0.142	0.1248
Control sample 2	0.153	0.1379
Control sample 3	0.137	0.1211
Control sample 4	0.114	0.0986
Control sample 5	0.112	0.0970
Control sample 6	0.133	0.1176
Average	**0.132**	**0.1162**
Rel. Std. Dev.	**12.2%**	**13.63%**

Microbial growth in hydrolysate flasks

One colony was detected on the fifth control sample's plate. One colony was also detected on one of the plates with hydrolysate with added levulinic acid. No colonies were visible on remaining plates. This indicates that the number of culturable microorganisms on YPD plates was less than 10 mL^{-1}.

Composition of the liquid fraction from hydrolysates

In Figure 19 a summary of the change in the concentration of investigated compounds in the liquid fraction throughout the hydrolysis can be seen for the control samples. Glucose, furfural, and ethanol changed noticeably during the hydrolysis experiments. Glucose increased over time from an average initial concentration of 12.59 ± 0.30 g L^{-1} to and average final concentration of 28.28 ± 0.58 g L^{-1} (Figure 19). Ethanol however was not detected in the control samples and will be mentioned together with furfural down below.

The relative standard deviation for furfural increased over time for most hydrolysis experiment. This correlated with a decrease in furfural concentrations. There was no clear trend other than a decrease in furfural concentrations over time. However, for the hydrolysis experiments with added xylose, the concentration of furfural increased with time. For the remaining furfural in all experiments, see Figure 20.

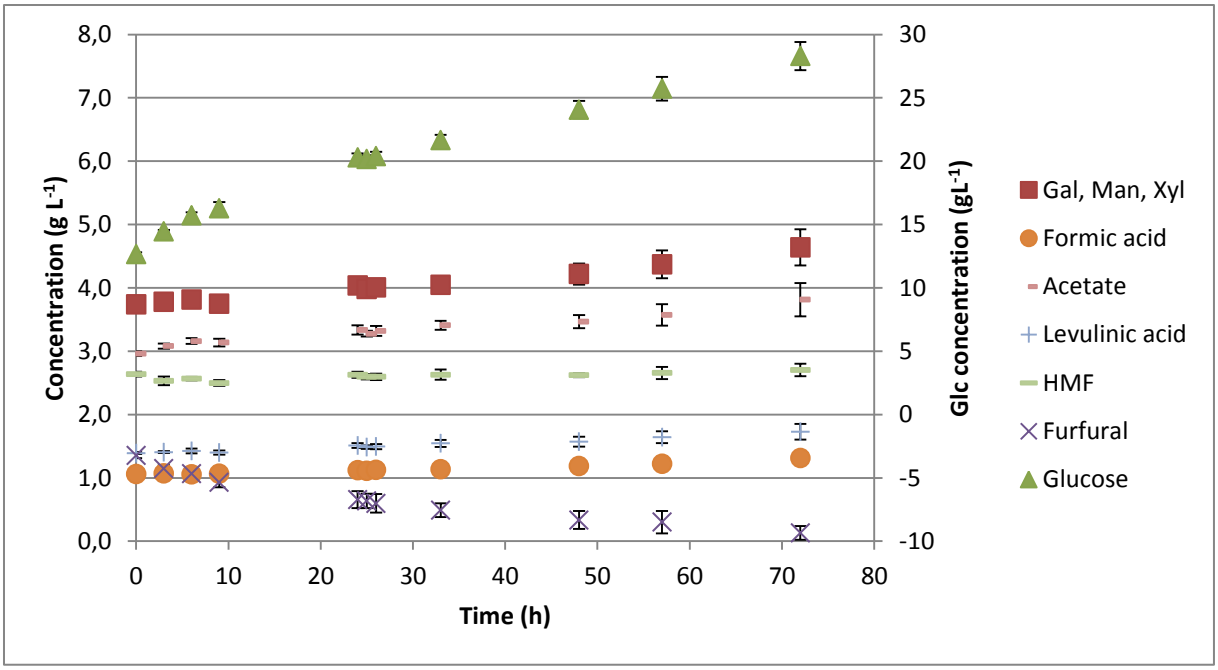

Figure 18 – Concentrations of the different inhibitors for the control samples (n=6) in the liquid fraction. Glucose concentration is shown using the right y-axis while the remaining compounds are displayed using the left y-axis. Galactose, mannose and xylose are represented as one item due to co-elution of the peaks. Error bars denotes 1 standard deviation in each direction of the mean.

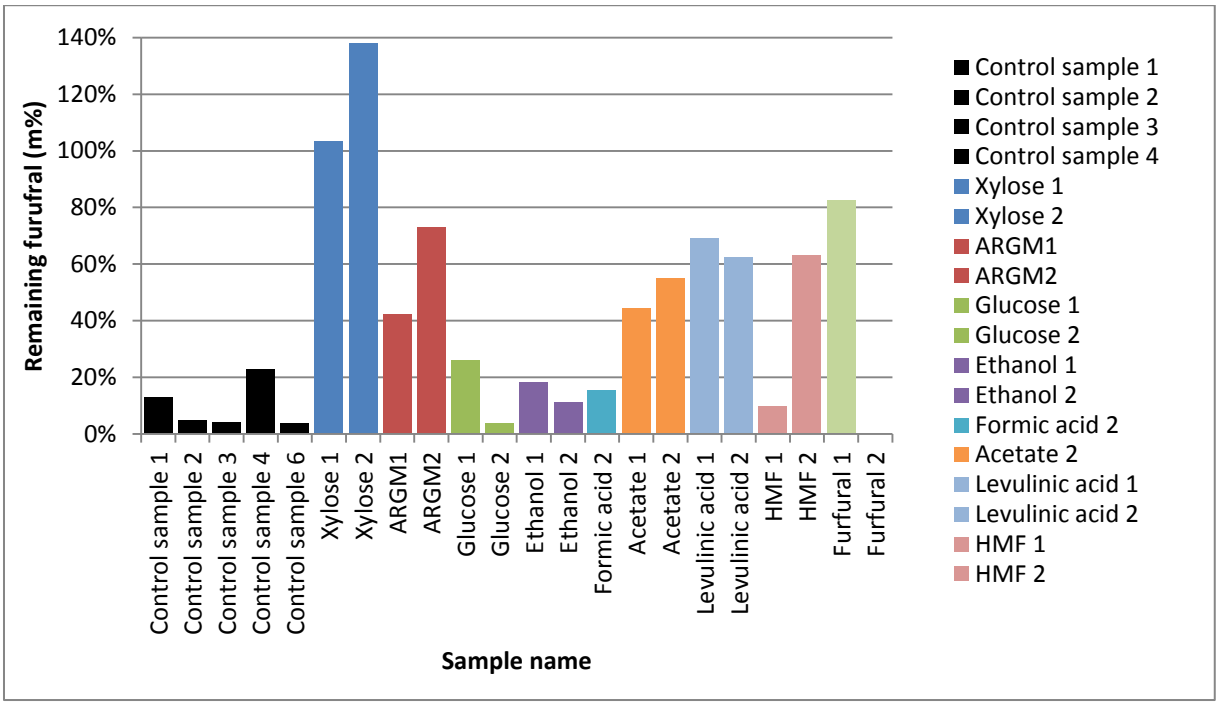

Figure 20 – Remaining furfural concentration after 72 hours of hydrolysis for each hydrolysis experiment as a percentage of initial concentration. Numbers indicate duplicate index. Control sample 5 and Formic acid 1 are not shown due to the data points being unreliable. Concentration for furfural for sample furfural 2 were below detection limit (<67 mg L^{-1}) and is thus presented as zero.

Ethanol was detected in samples with added xylose, ARGM, glucose or ethanol which can be seen in Figure 21 and Figure 22. The samples xylose 2, ARGM 1, glucose 1 and glucose 2 increased rapidly in ethanol concentration during the first 12 hours before peaking at the 9th,

6th, 9th and 26th hour respectively. The ethanol concentrations in xylose 2 and glucose 1 then decreased below the detection limit until the end of hydrolysis while ARGM 1 and glucose 2 stabilized around 1-2 g L^{-1}. Ethanol concentrations in xylose 1 and ARGM 2 increased rapidly in the first 12 hours and then stabilized around 2 g L^{-1}. The ethanol concentration in the samples with added ethanol decreased over time to almost zero (Figure 22).

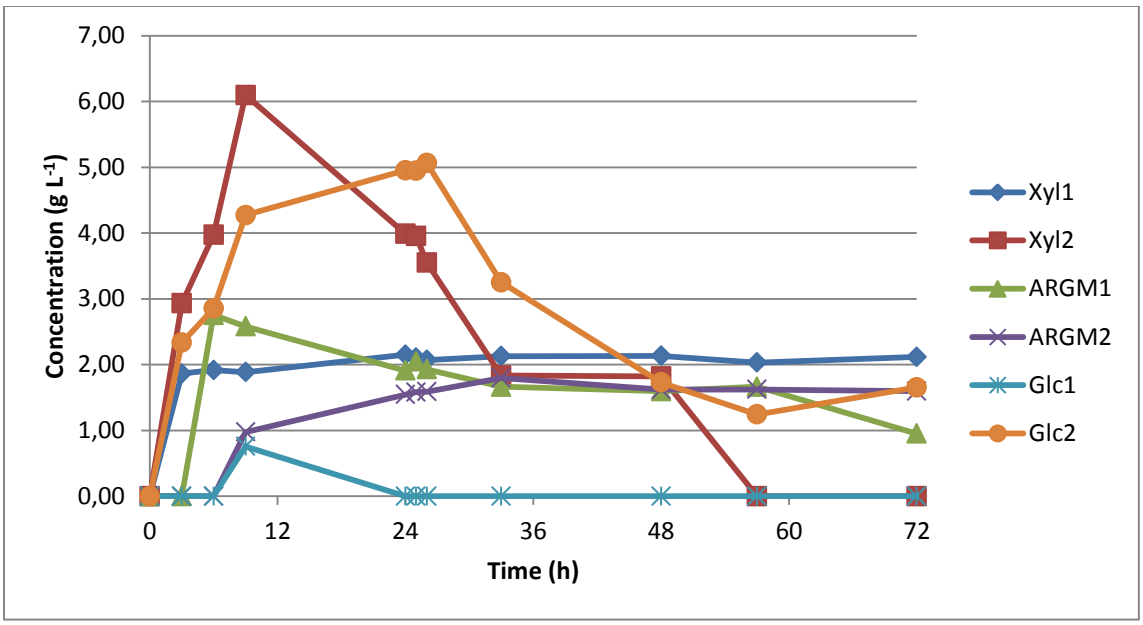

Figure 21 - Ethanol concentration over time for the samples with added xylose, ARGM and glucose. Data values depicted as zero are lower than the detection limit (<0.75 g L^{-1}).

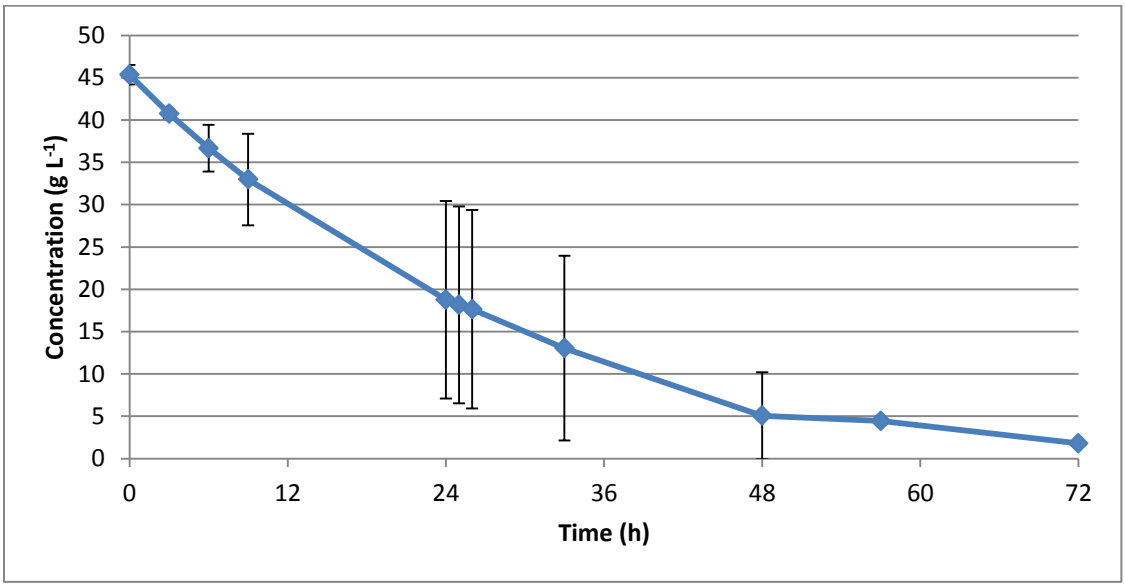

Figure 22 – Average ethanol concentration in the liquid fraction for hydrolysis samples with added ethanol. Error bars denote 1 standard deviation in each direction from the mean (n=2).

Glucose productivity rates and yields

Figure 23 displays the average estimated average decrease in glucose productivity between 6 h and 26 h after hydrolysis start for each of the nine different hydrolysis experiments and the control samples. The samples with added glucose had a significantly lower decrease in

productivity as compared with samples with added furfural, formic acid, acetate, and ethanol. Samples with added formic acid had significantly higher decrease in productivity as compared to the control samples.

The average maximal productivity can be viewed in Figure 24. The samples with added ethanol showed one of the lowest maximal productivities and were significantly lower than the control samples. There were no significant differences between the glucose productivity in all other samples.

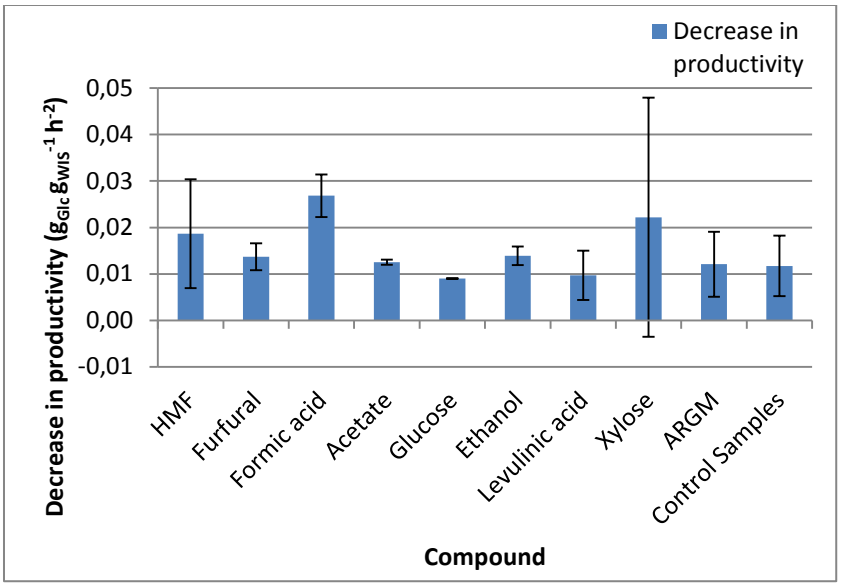

Figure 23 – The average estimated average decrease in glucose productivity ($g_{Glc}\,g_{WIS}^{-1}\,h^{-1}$) per hour. Error bars denotes one standard deviation in each direction from the mean (n=2).

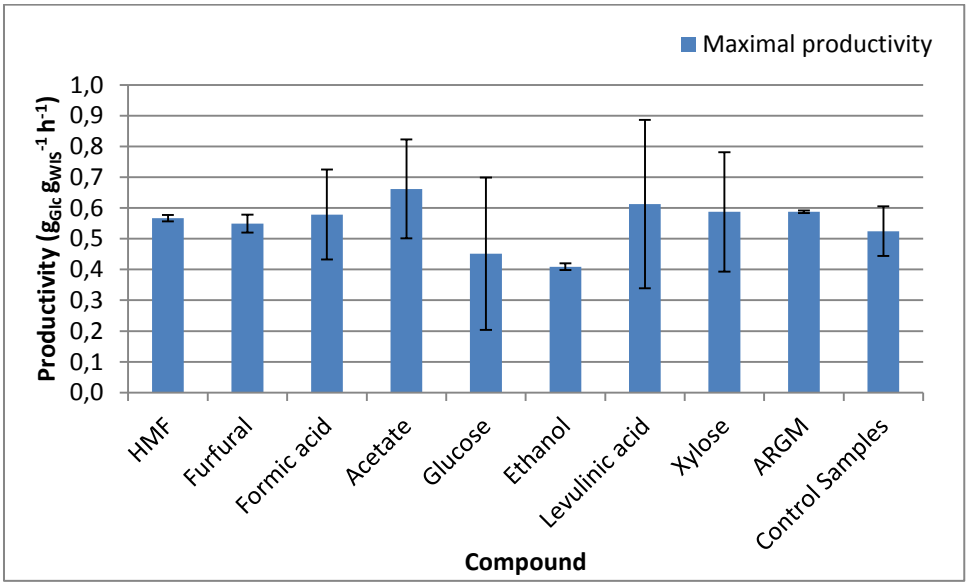

Figure 19 – The average maximum productivity for any time point t_j, using neighboring time points t_{j-1} and t_{j+1} for each hydrolysis experiment. Error bars denotes one standard deviation in each direction from the mean (n=2).

The average amount of glucose produced and the three glucose yields, mass glucose produced per mass cellulose present at hydrolysis start, mass glucose produced per mas WIS present at hydrolysis start and mass glucose produced per mass slurry present at hydrolysis start (see p. 21), are presented in Figure 25. Samples with added acetate had a significantly lower yield compared with the control samples. Remaining samples' yields did not differ significantly from that of the control samples'.

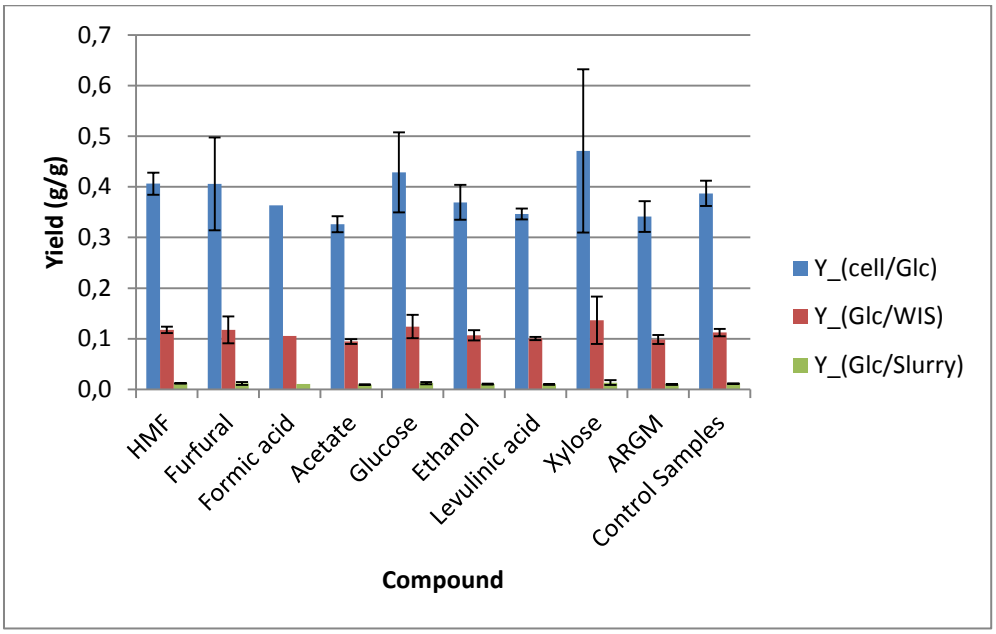

Figure 20 – The yields of glucose on cellulose, WIS and total slurry for each hydrolysis experiment: Grams glucose produced per gram cellulose at the start of hydrolysis ($Y_{Glc/cell}$), grams glucose produced per gram WIS at the start of hydrolysis ($Y_{Glc/WIS}$), grams glucose produced per gram slurry at the start of hydrolysis ($Y_{Glc/Slurry}$). Only one data point was available for the formic acid yields, hence no error bars. Error bars denotes one standard deviation in each direction from the mean (n=2).

The yields of glucose produces as a fraction of the total mass of releasable sugars are Figure 26. Samples with added acetate showed significant difference with the samples with the control samples. Remaining samples' yields did not differ significantly from that of the control samples'.

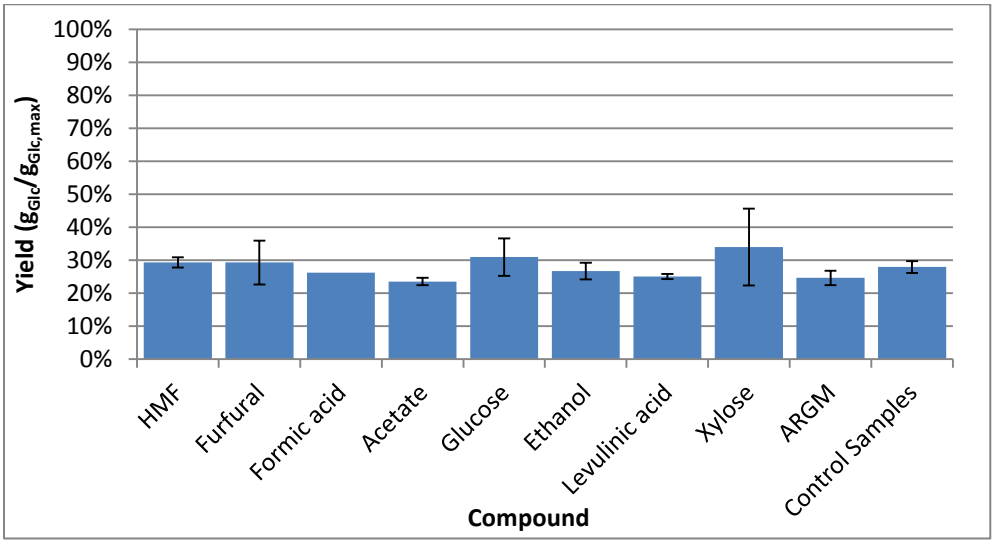

Figure 26 – The percentage of the theoretical maximum yield ($g_{Glc,max}$ = 5.02 g). Only one data point was available for the formic acid yields, hence no error bars. Error bars denotes one standard deviation in each direction from the mean (n=2).

Statistical analysis

The Mann–Whitney U test showed no significant difference for any set of samples for $\alpha = 0.05$, where α being the significance level. The acetate samples were significantly different for $\alpha = 0.1$.

Enzymatic activity and enzyme assay calibration curves

Figure 27 and Figure 28 presents the calibration curves for the enzyme assay for each of the two plate readers (Spectro star & FLUOstar) used. Linear regression curves were fitted to each plot. The differences between the two measurements are very small. The enzymatic activity was found to be 164.1 FPU mL^{-1} ± 3.8 FPU mL^{-1}.

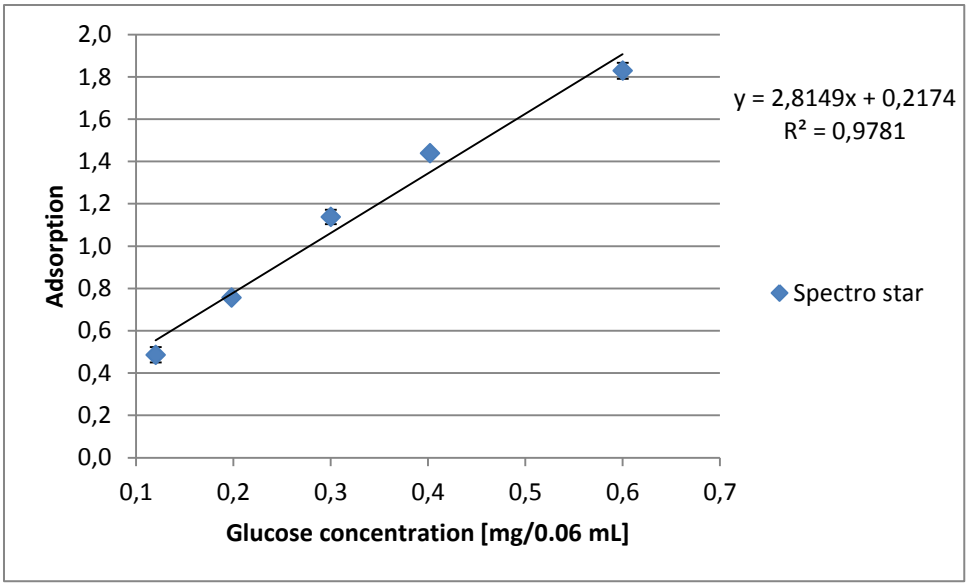

Figure 21 – Calibration curve for glucose standards analyzed at 540 nm using the Spectro star nano BMG Labtech plate reader. Error bars shows 1 standard deviation in each direction from the mean (n=3). The y-axis shows adsorption and the x-axis shows glucose concentration (mg/0.06 mL).

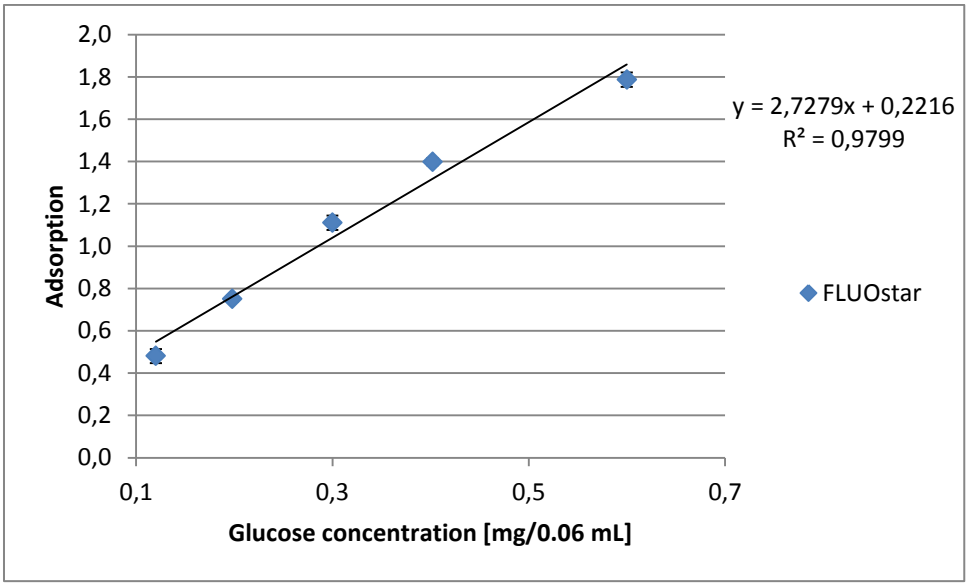

Figure 22 - Calibration curve for glucose standards analyzed at 540 nm using the BMG FLUOstar OMEGA plate reader. Error bars shows 1 standard deviation in each direction from the mean (n=3). The y-axis shows adsorption and the x-axis shows glucose concentration (mg/0.06 mL).

Discussion

The hydrolysis system

The hydrolysis system developed proved to be durable by processing 32 individual experiments over four consecutive weeks. Thanks to its parallelization capabilities it was easy adjusting the number of samples to run and could be used for one shake flask up to sixteen. Glucose concentrations for the control samples had a relative standard deviation after 72 h of hydrolysis of 6.4% (Figure 19), which is within acceptable limits for a material as heterogeneous as the one investigated here. Improvements to the system can however be made. A convenient method for matching inlet and outlet tubing with appropriate shake flasks for untroublesome logistics while setting up an experiment has yet to be envisioned. An improved sampling method also needs to be developed which does not require the removal of the rubber stoppers and hence introduces potential contamination.

Effectiveness of analysis methods and analysis method development

Reasons for not relying on the UV/VIS adsorption chromatogram data for characterization of the material were several. The UV/VIS detector did not detect as many compounds as the RI detector which could also identify glycerol, formic acid, ethanol, and vanillin. Comparing the combined concentration galactose, mannose, and xylose that the UV/VIS detector reported (37 g L^{-1}) with the data from the IC (15 g L^{-1}) strongly indicated that the UV/VIS data was not trustworthy. Furthermore, the relative standard deviations were on the whole larger for the investigated compounds when analyzed with the UV/VIS on the HPLC as compared with the IC.

Regardless of using the UV/VIS or RI detector, ferulic and trans-ferulic acid could not be found. It is possible that ferulic acid, because it has a similar chemical structure to vanillin, elutes far beyond furfural, possibly beyond 2h. While it would be useful to know the concentrations of ferulic acid in the material the possibly very long HPLC run times would come at the cost of adequate sample size for statistical basis. This reasoning was already applied for vanillin, and it is partially why it is not included in the analysis of the hydrolysis samples. Further reasons for excluding vanillin was that the concentrations of it were below the quantification limit in all samples.

Due in part to complications with IC analysis, alternative analysis methods using HPLC were investigated. Potential carbonization by trace amounts of atmospheric CO_2 of the IC eluent might have led to a drift of the peaks since the carbonate ions would bind to the column and decrease the elution time of the analytes. This made eluent changes throughout the analysis necessary, repeated runs of standards and extra post analysis treatment of the data to account for the drift. It furthermore made manual peak processing necessary which also exacerbated the time needed. This prompted the investigation of the Rezex Pb column.

Despite using recommended methods from literature for sugar separation, reproducibility of the results was not possible. The column has restrictive method alternatives. For the mobile phase, it is recommended to avoid acids, bases, non-lead salts, metal ions, ACN above 30% or other organic modifiers above 5% [38]. This does not leave many common solutions, except water. High temperatures and water as the mobile phase gave the best peak separation. The eluent flow rate did not affect peak separation appreciable although it could be argued that slower speeds led to slightly better separation. A balance must however be struck between the time of analysis and the degree of separation. Temperatures above 80°C could not be tested due to the limitation of the HPLC system. It is however not believed that this would result in any, for this project, useful results. As can be seen in Figure 9, arabinose has a very strong response and co-elutes heavily with mannose. This means that even very small amounts of arabinose in any hydrolysate sample will most likely obfuscate the mannose concentration, which is also very low in the pretreated material (Figure 15). The possibility of creating a clear baseline separation between xylose and galactose is made difficult by rhamnose, which can be seen in Figure 10. The methods developed so far can however be used as an easy to use method for qualitative identification in samples with 4-5 different sugars.

The Kinetex F5 column promised substantially cut analysis time and the identification of organic acids. While the method was faster, only the aromatic compounds and the positive control, sorbic acid, could be identified despite running 67 separate samples under many different conditions and indications to the contrary (see Table 13 in the appendix and [32]). The reasons for these results eludes the author. The same acid standards used for this column was successfully used later on the Rezex ROA column on the same HPLC. This means that the result can neither be because the detector cannot detect the compounds, nor that the standard solutions are faulty. If the analytes eluted much later than any program, one would still expect to see out of place peaks in consecutive chromatographs. If they were not retained at all, they should elute with the injection front which will still be visible when comparing to a blank. This was not observed. The only conclusion remaining is that the acid analytes bound completely to the column and were never washed out.

The calibration curves for HMF and furfural had a much steeper slope with over a magnitude in difference as compared to the calibrations curves derived with the Rezex ROA column. This means that HMF and furfural at very low concentrations can be analyzed on the Kinetex F5 column. The unidentified peaks in Figure 4 pose a conundrum to the author. These peaks emerged whenever a gradient elution was applied, but never when an isocratic method was used nor when an abrupt shift in the water/ACN ratio was made during the run. These peaks emerge even if the sample used is MilliQ water. Consulting with experts in the field of HPLC analysis did not yield an explanation either.

An interesting finding is that the peak intensity of vanillin was much higher using the Kinetex column with the PDA detector as opposed to the Rezex ROA with RI detection. This leaves open the possibility of quantifying vanillin in the future.

The reason for developing the method for the Rezex ROA column on the gradient HPLC was in the event of a successful method development for the Rezex Pb column on the isocratic HPLC and an unsuccessful method development for the Kinetex F5 column. This would allow for parallelization of the analysis and keep analysis duration down, since you could analyze sugars on the isocratic HPLC with the Rezex Pb column, and acids and aromatics with the Rezex ROA column on the gradient HPLC simultaneously. Hence it would not be a loss if sugars were not detected with the PDA detector. However, it is a problem that ethanol is not detected, partly because it serves as an indicator of contamination of a fermentative microorganism in hydrolysate samples, but mainly because it is of uttermost importance that intentionally fermented slurry can be assessed for its ethanol concentration in the future.

Effects of pretreatment parameters on slurry composition

The composition of the material was consistent with data from Räisänen et al. and similar to that of bark with cellulose content around 30m% of the dry weight and hemicellulose content of about 10m% (Figure 17 and 17) [22]. Since the cross sectional area and thus the fraction of stem wood decreases quadratic with decreasing radius it is reasonable that the cellulose and hemicellulose fractions are much closer to bark, needles and branches than to stem wood in branches and tips.

Different pretreatment conditions had an effect on the composition of the material. The amount of releasable sugars peaked for a severity factor around 4.07. Higher severity factor resulted in lower amounts of releasable sugars than did lower severity factors (Figure 12 and Figure 13). This aligns with what one would expect. A harsher pretreatment process leads to more sugar degradation into inhibitors and lower amount of releasable sugars. The preferred severity factor for a pretreatment should however also be weighed against the amount sugars released, since materials with higher amounts of sugars released will lead to lower hydrolysis requirements and lower enzyme costs. As seen in Figure 15, the concentration of sugars in the liquid fraction did not significantly increase with a severity factor higher than 4.07, which was the case for MAT.lB.110. In fact, the pretreatment for material MAT.lB.105 with a severity factor of 3.91 likely contains the highest concentration of sugars in the liquid fraction out of all the materials. With the idea that a severity factor of roughly 4.0 is optimal it is tempting to argue that MAT.lB.103 with a severity factor of 4.20 and the lowest amount of inhibitors, as seen in Figure 14, has so because 4.20's proximity to 4.0. It is however hard to explain why this would be the case. Materials subject to a lower severity factor has similar inhibitor concentrations as materials with higher severity factor. If higher severity factors cause more degradation of sugars, then inhibitor concentrations should increase, which they do not. And if one argues that higher severity factors also leads to more degradation of the inhibitors into carbon dioxide and water which counters the increased production of inhibitors from sugar degradation, then inhibitor concentrations should remain stable throughout, which they do not. There are also uncertainties involving the accuracy of the severity factor, as heating of material during the pretreatment might not have happened uniformly (C.J. Franzén, personal communication). It would be advisable to do more pretreatments in the severity factor region of 4.0-4.2 to obtain more statistically certain data.

Effect of inhibitors on hydrolysis rates and yields

The main conclusions that can be drawn from the hydrolysis experiments are that the addition of different compounds had no significant effects on the hydrolysis rates or yields. Formic acid was the only compound that significantly affected the productivity at a 95% significant level (Figure 23). At the same level of significance, only ethanol affected the maximal productivity (Figure 24), and only acetate affected the yields (Figure 25 and Figure 26). This is not to say that remaining compounds are not inhibitory. It is rather more likely that the enzyme is saturated with inhibitors to the extent that adding more inhibitors will not decrease the hydrolysis rate further. It could also be the case that the perturbation of the hydrolysis inhibitor concentration was not large enough to make a difference to the hydrolysis rate. According to Jing et al., 25 g L^{-1} of formic acid resulted in a 25% drop in glucose produced while 3 g L^{-1} of HMF and furfural lead to a 5-10% drop in glucose produced [39]. This can be compared to the initial concentrations of 2.25 g L^{-1} of formic acid, 4.36 g L^{-1} of HMF, and 1.89 g L^{-1} of furfural in their respective hydrolysis samples at the start of hydrolysis in this project. Only HMF was at a concentration where minor inhibition would be expected, and due to the low number of replicates used, this effect cannot be observed. It should be noted that any real but small effect will be hidden by the relatively large errors, which stems from the low number of replicates.

The concentrations of inhibitor were however not chosen to necessarily cause inhibition. They were chosen to illustrate hydrolysis conditions under a realistic worst case scenario. A robust glucose production independent of changes in inhibitor concentrations on this scale means that pretreatment conditions can be varied more freely and thus allow for other aspects apart from inhibitor production to be addressed such as higher degree of disintegration of the material. This would increase the available surface area and thus the hydrolysis rate. It would however be recommended to perform a positive control and increase all the inhibitor concentrations as done in this project but in the same sample.

The decrease in furfural, the presence of ethanol and the results from the YPD plates are all tied together by the question of potential microorganism contamination. The simplest and least controversial hypothesis would be a common yeast contamination that is metabolizing furfural to furfuryl alcohol and glucose to ethanol anaerobically [40]. The enzyme responsible for these two reactions, alcohol dehydrogenase, is only moderately inhibited by furfural [41]. One would hence expect to see furfural consumption and ethanol production in contaminated experiments. One would also expect to see microbial growth on the YPD plates. Glucose consumption on the other hand might not be noticeable because the net production rate of glucose is the sum of the hydrolysis rate and potential microorganism consumption of glucose for ethanol production and growth. In all samples which produced ethanol a decrease in furfural concentrations was observed, except in samples with added xylose. However, remaining samples also had decreasing furfural concentrations similar to those in the samples with ethanol production. Furthermore, since consumption of furfural is coupled to glucose consumption and thus by extension ethanol production because of the need to maintain a nicotinamide adenine dinucleotide (NADH) balance, one would expect samples with the

highest amount of ethanol produced to also have the largest decrease in furfural. This is not the case as the samples with added xylose, which are among the samples with most ethanol produced, also are the ones with no decrease in furfural concentrations. Lastly, no growth was visible on the YPD plates, which also argues against the proposed hypothesis. In conclusion, while there are some indications that some of the samples might have been contaminated by a common yeast, there are several indications against such a hypothesis as well. Good scientific and skeptical practice dictates that one should err on the side of caution and falsify the hypothesis, since a good hypothesis should be able to explain all the available data, so that is therefore done. With a replicate number as low as the one in this study that is not possible, as the statistical basis for any conclusions based on indirect observations, such as the ones discussed above, is very weak. Alternative hypotheses involving less common microbiological contaminants would require even stronger evidence than the ones available here to be accepted.

Blind spots

The author acknowledges that there are several blind spots in this project. The three assumptions made in the hydrolysis experiments subsection for calculating the amount of glucose produced introduces errors; especially the assumption that the WIS stays constant. Measurements of the WIS for each time point would help understanding the kinetics of the hydrolysis reaction and get more accurate yields and productivity estimates. The solid fraction from the hydrolysis was not analyzed, and thus its effect on the glucose production and interaction with the liquid fraction remains unknown. It should be pointed out however that most inhibitors are highly water soluble and so from the perspective of investigating the inhibitory effect on the hydrolysis rate, this gap in the knowledge of the composition of the hydrolysate is not detrimental to the results or the conclusions drawn. The biggest blind spot could however be the lignin. Looking at Figure 16 and Figure 17, the average holocellulose content per g_{WIS} is roughly 0.33 g. This means that as high as 60%-70% could be lignin and extractives, which together with its degradation products are known hydrolysis and fermentation inhibitors [26, 30, 31]. It is not unlikely that lignin and lignin derivatives has been the main hydrolysis rate limiting factor. It is recommended that future studies incorporate effects of lignin on the hydrolysis and fermentation rates.

Conclusions and outlook

In conclusion, a reliable parallel shake flask hydrolysis system has been developed to be able to investigate perturbations to the hydrolysis process of Norway spruce residues from branches, tips and needles by the addition of compounds identified in the scientific literature as inhibitors. Method development for the three columns Kinetex F5, Rezex ROA and Rezex Pb has laid a foundation for future method development that might result in large time savings for the analysis of both pretreated and hydrolyzed spruce residue material. The holocellulosic fractions were consistent with the literature and it was concluded that a pretreatment severity factor lower than 4.00 will likely produce the highest amount of releasable sugars. Despite some indication that increased ethanol and acetate concentrations decreases the hydrolysis rate and yield respectively it seems in a broader scope as if changing inhibitor concentrations within realistic spans does not affect productivity and yield which indicates a recalcitrant material with respect to hydrolysis with low glucose hydrolysis yields (~30% of the theoretical maximum). Due to the broad lack of statistical differences in inhibitory effects, there are not enough grounds for recommending any specific recommendations for a future SSCF process. This also means that, based on these results, it is likely that the inhibitors investigated can be grouped and modeled as one compound for future kinetic simulations.

Recommendations for future studies of this material and the hydrolysis process are to develop faster analysis methods that can also measure the complex sugar profiles with accuracy and reliability, perform a positive control experiment with all investigated inhibitors at elevated concentrations as this would possibly exclude their contribution to productivity and yield, a negative control experiment without the addition of enzymes to investigate if ethanol and furfural change over the time period, screening for lactic acid bacteria using MRS agar, and the investigation of lignin and lignin derivatives as inhibitors on hydrolysis as the lignin most likely makes up the major part of the material. It is also highly recommended that the hydrolysis experiments preformed in this project are repeated to increase the statistical basis for this thesis conclusion.

Acknowledgments

I would like to thank my examiner Carl Johan Franzén and supervisor David Benjamin Nickel for assisting and guiding me throughout this project. They have both managed to inspire and support me as well as keeping me grounded and focused which has meant a lot. I would also like to especially thank lab engineer Julia Lind for her support during HPLC column method development and for answering all lab related questions I have had. Appreciation also extends to Joshua Mayers, Julia Wilke, Marlous Van Dijk, Jeroen Maertens, Fábio Luis Da Silva Faria Oliveira, and Rakesh Koppram for answering smaller questions and giving tips on laborative work. They have all saved me several hours of work and cheered my up during late evenings, early mornings and well-deserved coffee breaks.

Sources

1. C. B. Field, V.R.B., M. D. Mastrandrea et.al., *Summary for Policymakers*, in *Climate Change 2014: Impacts, Adaptation, and Vulnerability. Part A: Global and Sectoral Aspects. Contribution of Working Group II to the Fifth Assessment Report of the Intergovernmental Panel on Climate Change*, C.B. Field, V.R. Barros, D.J. Dokken, K.J. Mach, M.D. Mastrandrea,, M.C. T.E. Bilir, K.L. Ebi, Y.O. Estrada, R.C. Genova, B. Girma, E.S. Kissel, A.N. Levy, S. MacCracken,, and a.L.L.W. P.R. Mastrandrea, Editors. 2014, International Panel on Climate Change: https://ipcc.ch/report/ar5/wg2/. p. 34.
2. L. V. Alexander, S.K.A., N. L. Bindoff et.al., *Summary for Policymakers*, in *Climate Change 2013: The Physical Science Basis. Contribution of Working Group I to the Fifth Assessment Report of the Intergovernmental Panel on Climate Change*, T.F. Stocker, D. Qin, G.-K. Plattner, M. Tignor, S.K. Allen, J. Boschung, A. Nauels, Y. Xia, V. Bex and P.M. Midgley, Editor. 2013, International Panel on Climate Change: https://www.ipcc.ch/report/ar5/wg1/. p. 28.
3. Koçar, G. and N. Civaş, *An overview of biofuels from energy crops: current status and future prospects.* Renewable and Sustainable Energy Reviews, 2013. **28**: p. 900-916.
4. B. Flach, S.L., K. Bendz, *EU Annual biofuels Report*, in *Biofuels Annual*. 2010, Global Agricultural Information Network: USDA Foreign Agricultural Service. p. 38.
5. B. Flach, S.L., M. Rondon et. al., *EU Biofuels Annual 2016*, in *Biofuels Annual*. 2016, Global Agricultural Information Network: USDA Foreign Agricultural Service. p. 42.
6. Wang, L., J. Littlewood, and R.J. Murphy, *Environmental sustainability of bioethanol production from wheat straw in the UK.* Renewable and Sustainable Energy Reviews, 2013. **28**: p. 715-725.
7. Borrion, A.L., M.C. McManus, and G.P. Hammond, *Environmental life cycle assessment of bioethanol production from wheat straw.* Biomass and Bioenergy, 2012. **47**: p. 9-19.
8. Lim, J.S., et al., *A review on utilisation of biomass from rice industry as a source of renewable energy.* Renewable and Sustainable Energy Reviews, 2012. **16**(5): p. 3084-3094.
9. Huang, H.-J., et al., *A review of separation technologies in current and future biorefineries.* Separation and Purification Technology, 2008. **62**(1): p. 1-21.
10. Naik, S.N., et al., *Production of first and second generation biofuels: a comprehensive review.* Renewable and sustainable energy reviews, 2010. **14**(2): p. 578-597.
11. Sims, R.E., et al., *An overview of second generation biofuel technologies.* Bioresource technology, 2010. **101**(6): p. 1570-1580.
12. Chakravorty, U., et al., *Long-Run Impact of Biofuels on Food Prices.* The Scandinavian Journal of Economics, 2017. **119**(3): p. 733-767.
13. Rulli, M.C., et al., *The water-land-food nexus of first-generation biofuels.* Scientific reports, 2016. **6**: p. 22521.
14. Mohr, A. and S. Raman, *Lessons from first generation biofuels and implications for the sustainability appraisal of second generation biofuels.* Energy policy, 2013. **63**: p. 114-122.
15. Deswarte, F.E., et al., *The fractionation of valuable wax products from wheat straw using CO 2.* Green Chemistry, 2006. **8**(1): p. 39-42.
16. Pauly, M. and K. Keegstra, *Cell-wall carbohydrates and their modification as a resource for biofuels.* The Plant Journal, 2008. **54**(4): p. 559-568.
17. Naik, S., et al., *Characterization of Canadian biomass for alternative renewable biofuel.* Renewable energy, 2010. **35**(8): p. 1624-1631.
18. Shimada, K., S. Hosoya, and T. Ikeda, *Condensation reactions of softwood and hardwood lignin model compounds under organic acid cooking conditions.* Journal of wood chemistry and technology, 1997. **17**(1-2): p. 57-72.
19. Brebu, M. and C. Vasile, *Thermal degradation of lignin—a review.* Cellulose Chemistry & Technology, 2010. **44**(9): p. 353.
20. Willför, S., et al., *Polysaccharides in some industrially important softwood species.* Wood Science and Technology, 2005. **39**(4): p. 245-257.
21. Krogell, J., et al., *Extraction and chemical characterization of Norway spruce inner and outer bark.* Nord Pulp Pap Res J, 2012. **27**(1): p. 6-17.
22. Räisänen, T. and D. Athanassiadis, *Basic chemical composition of the biomass components of pine, spruce and birch.* 2013.
23. Timell, T., *Isolation of galactoglucomannans from the wood of gymnosperms.* Tappi, 1961. **44**: p. 88-96.

24. Dietrichs, H., et al., *Untersuchungen über die Kohlenhydrate der Rinden einheimischer Holzarten.* Holzforschung-International Journal of the Biology, Chemistry, Physics and Technology of Wood, 1978. **32**(2): p. 60-67.
25. Alvira, P., et al., *Pretreatment technologies for an efficient bioethanol production process based on enzymatic hydrolysis: a review.* Bioresource technology, 2010. **101**(13): p. 4851-4861.
26. Talebnia, F., D. Karakashev, and I. Angelidaki, *Production of bioethanol from wheat straw: an overview on pretreatment, hydrolysis and fermentation.* Bioresource technology, 2010. **101**(13): p. 4744-4753.
27. Jeffries, T. and Y.-S. Jin, *Metabolic engineering for improved fermentation of pentoses by yeasts.* Applied Microbiology and Biotechnology, 2004. **63**(5): p. 495-509.
28. Westman, J.O., et al., *Sustaining fermentation in high-gravity ethanol production by feeding yeast to a temperature-profiled multifeed simultaneous saccharification and co-fermentation of wheat straw.* Biotechnology for biofuels, 2017. **10**(1): p. 213.
29. Chang, V.S. and M.T. Holtzapple. *Fundamental factors affecting biomass enzymatic reactivity*. in *Twenty-first symposium on biotechnology for fuels and chemicals*. 2000. Springer.
30. Vohra, M., et al., *Bioethanol production: feedstock and current technologies.* Journal of Environmental Chemical Engineering, 2014. **2**(1): p. 573-584.
31. Fischer, C.R., D. Klein-Marcuschamer, and G. Stephanopoulos, *Selection and optimization of microbial hosts for biofuels production.* Metabolic engineering, 2008. **10**(6): p. 295-304.
32. Kinetex, *New Kinetex F5 - HPLC/UHPLC Core-Shell Columns*. Phenomenex.
33. McGinley, M., *Optimizing the Analysis of Sugar Alcohol Excipients in Pharmaceutical Tablet Formulations Using Rezex™ Ion Exclusion HPLC Columns.* LC GC Magazine-North America-Solutions forSeparation Scientists, 2011. **63**: p. 48.
34. Pedersen, M. and A.S. Meyer, *Lignocellulose pretreatment severity–relating pH to biomatrix opening.* New biotechnology, 2010. **27**(6): p. 739-750.
35. Sluiter, A., et al., *Determination of structural carbohydrates and lignin in biomass.* Laboratory analytical procedure, 2008. **1617**: p. 1-16.
36. Xiao, Z., R. Storms, and A. Tsang, *Microplate-based filter paper assay to measure total cellulase activity.* Biotechnology and Bioengineering, 2004. **88**(7): p. 832-837.
37. Adney, B. and J. Baker, *Measurement of cellulase activities.* Laboratory analytical procedure, 1996. **6**: p. 1996.
38. Phenomenex, *Rezex Carbohydrate and Organic Acid LC: Rezex HPLC Columns Tips for Care and Use*, in *http://az621941.vo.msecnd.net/documents/a5e9b9b8-8a48-4bc8-b17b-e2a1e46648f8.pdf*, Phenomenex, Editor. 2018.
39. Jing, X., X. Zhang, and J. Bao, *Inhibition performance of lignocellulose degradation products on industrial cellulase enzymes during cellulose hydrolysis.* Applied biochemistry and biotechnology, 2009. **159**(3): p. 696.
40. Horváth, I.S., et al., *Effects of furfural on the respiratory metabolism of Saccharomyces cerevisiae in glucose-limited chemostats.* Applied and environmental microbiology, 2003. **69**(7): p. 4076-4086.
41. Modig, T., G. Liden, and M.J. Taherzadeh, *Inhibition effects of furfural on alcohol dehydrogenase, aldehyde dehydrogenase and pyruvate dehydrogenase.* Biochemical Journal, 2002. **363**(3): p. 769-776.

Appendix

Standards and stocks Table

Table 11 – Overview of most standards and stocks used during the project. Standards labeled "IC" were used for IC, standards labeled "HPLC" were used for HPLC and stocks labeled "hydrolysis" were used during the preparation of samples for the hydrolysis experiments. "Standard" is abbreviated "std". "Without" is abbreviated "w/o".

Standard/stock Name	Substance name	Concentration (g/L)
IC standard mix	Sorbitol	0.1
	Mannitol	0.1
	Arabinose	0.1
	Rhamnose	0.1
	Galactose	0.1
	Glucose	0.1
	Xylose	0.1
	Fructose	0.009
Mannose IC std	Mannose	0.1
Mannose IC recovery std	Mannose	0.340
Galactose IC recovery std	Galactose	0.173
Glucose IC recovery std	Glucose	1.384
Xylose IC recovery std	Xylose	0.208
Arabinose IC recovery std	Arabinose	0.092
Glucose HPLC std	Glucose	25
Galactose HPLC std	Galactose	25
Mannose HPLC std	Mannose	25
Xylose HPLC std	Xylose	25
Ethanol HPLC std	Ethanol	25
Glycerol HPLC std	Glycerol	5
HMF HPLC std	HMF	10
Furfural HPLC std	Furfural	10
Vanillin HPLC std	Vanillin	2.5
Levulinic HPLC acid std	Levulinic acid	2.5
Ferulic acid HPLC std	Ferulic acid	0.5
Acetate HPLC std	Sodium acetate*	12.5
Citrate HPLC std	Dihydrated sodium citrate*	15
Formic acid HPLC std	Formic acid	5
Trans-ferulic acid HPLC std	Trans-ferulic acid	1
HPLC Sugar mix std	Glucose	25
	Galactose	25
	Mannose	25
	Xylose	25
	Ethanol	25

	Glycerol	5
HPLC Acid mix 1 std	Levulinic acid	2.5
	Ferulic acid	0.5
	Sodium acetate*	12.5
	Dihydrated sodium citrate*	15
HPLC Acid mix 2 std	Levulinic acid	2.5
	Sodium acetate*	12.5
	Dihydrated sodium citrate*	15
	Formic acid	5
HPLC Aromatics mix std	HMF	10
	Furfural	10
	Vanillin	2.5
HPLC Arabinose std	Arabinose	25
HPLC Rhamnose std	Rhamnose	25
HPLC Sorbic acid std	Sorbic acid	1.5
HPLC New Sugar mix std	Glucose	25
	Galactose	25
	Mannose	25
	Xylose	25
	Arabinose	25
	Rhamnose	25
	Ethanol	25
	Glycerol	5
HPLC Supermix std	Levulinic acid	0.5
	Sodium acetate*	2.5
	Dihydrated sodium citrate*	3
	Formic acid	1
	HMF	2
	Furfural	2
	Vanillin	0.5
	Sorbic acid	1.5
HPLC Supermix w/o sorbic acid std	Glucose	12.5
	Galactose	12.5
	Mannose	12.5
	Xylose	12.5
	Ethanol	12.5
	Glycerol	2.5
	Levulinic acid	1.25
	Sodium acetate*	6.25
	Dihydrated sodium citrate*	7.5
	Formic acid	2.5

Acetate hydrolysis stock	Sodium acetate*	31.8
HMF hydrolysis stock	HMF	40.1
Furfural hydrolysis stock	Furfural	16.8
Levulinic acid hydrolysis stock	Levulinic acid	38.9
Glucose hydsolysis stock	Glucose	312
Xylose hydrolysis stock	Xylose	440
Formic hydrolysis acid stock	Formic acid	62.3
ARGM hydrolysis stock	Arabinose	21.1
	Rhamnose	14.0
	Galactose	50.2
	Mannose	120

* Concentrations for sodium acetate and dihydrated trisodium citrate are listed with respect to the ion of interest, i.e. concentration of acetate and concentration of citrate respectively.

Materials Table

Table 12 – Instruments used in this project.

Type of instrument	Name of instrument
Autoclave	Autoclave (Getinge, Sweden)
Centrifuge	Avanti J-26S XP Beckman coulter
Centrifuge	Beckman Coulter Allegra 25R benchtop centrifuge
HPLC System	Jasco LC-4000 Extreme
IC System	Dinoex ICS-3000 Reagent-Free™
Oven	BINDER drying and heating chamber
Plate reader	BMG FLUOstar OMEGA Microplate Reader
Plate reader	Spectro star nano BMG Labtech
Sample disruption system	Qiagen TissueLyser II
Shake incubator	IKA™ KS 4000 i Incubator Shakers

HPLC column method development experiments

Table 13 - Overview of the experiments conducted for the method development on the Kinetex F5 column for detection of aromatics and organic acids. Detection was made with the PDA detector at the listed wavelengths. All experiments where run with H_2O/ACN as a mobile phase at 0.6 mL min^{-1} at 30 °C unless otherwise noted. The percentages for isocratic runs in the 'Gradient program' column denote the fraction between water and ACN, respectively. Sample "T72S3" denotes control sample #3 after 72 hours of hydrolysis.

Kinetex F5 column method development experiments

Exp. #	Analytes	Dilution factor	Detection wavelengths	Runtime	Gradient program	Notes
1	Supermix	400	240 nm	60 min	A	*
2	Furfural	2000	240 nm	30 min	B	
	HMF					
	Acetate					
	Formic acid					
	Levulinic acid					

3	Sorbic acid	400	240 nm	30 min	A	*†
4	Sorbic acid	400	240 nm	30 min	B	
5	Sorbic acid	400	240 nm	10 min	Isocratic 65%/35%	**
6	Supermix	400	240 nm	10 min	Isocratic 65%/35%	
7	Supermix	400	240 nm	10 min	Isocratic 65%/35%	
					Isocratic 70%/30%	
					Isocratic 80%/20%	
					Isocratic 90%/10%	
8	Supermix	400	240 nm	15 min	C	
	Supermix w/o Sorb	1000				
	Acetate	2000				
	Formic acid					
	Levulinic acid					
	HMF					
	Furfural					
9	Supermix w/o Sorb	1000	240 nm	7 min	Isocratic 80%/20%	
	Acetate	2000				
	Formic acid					
	Levulinic acid					
	HMF					
	Furfural					
10	Supermix w/o Sorb	1000	240 nm	7 min	Isocratic 80%/20%	
	Acetate	400				
	Formic acid					
	Levulinic acid					
	HMF					
	Furfural					
11	Supermix	400	210 nm	7 min	Isocratic 80%/20%	
	Supermix w/o Sorb	1000				
	Acetate	2000				
	Formic acid					
	Levulinic acid					
	HMF					
	Furfural					
12	Supermix w/o Sorb	1000	210, 200, 220, 230 nm	7 min	Isocratic 80%/20%	
	Acetate	2000				
	Formic acid					
	Levulinic acid					
	HMF					
	Furfural					
13	T72S3	2000	210, 220, 230,	20 min	Isocratic 80%/20%	

			240 nm			
14	T72S3	80	240, 230, 220, 210 nm	20 min	Isocratic 80%/20%	
15	Furfural	50, 100, 200, 400, 800, 1600, 3200	240, 230, 220, 210 nm	7 min	Isocratic 80%/20%	
	HMF	800, 1600, 3200, 6400, 12800, 25600, 51200				
16	Furfural	6400, 12800, 25600, 51200	240, 230, 220, 210 nm	7 min	Isocratic 80%/20%	
	HMF	50, 100, 200, 400				

Gradient program A: 1 min w/ 95% 0.1v% H_3PO_4, decreasing H_3PO_4 to 65% over 6 minutes, 43 min w/ 65% 0.1v% H_3PO_4, 10 min w/ 95% 0.1v% H_3PO_4.

Gradient program B: 1 min w/ 95% H_2O, decreasing H_2O to 65% over 6 minutes, 14 min w/ 65% H_2O, 9 min w/ 95% H_2O.

Gradient program C: 2 min w/ 95% H_2O, 8 min w/ 80% H_2O, 5 min w/ 95% H_2O.

* Run with H_3PO_4/ACN.

** Run with at 20°C.

† Experiment not run.

Table 14 – Overview of the experiments conducted for the method development on the Rezex Pb column for detection of monosaccharides. All samples were analyzed with UV/VIS at 240 nm and RI. No samples were diluted from their stock concentrations (see Table 11) unless otherwise noted. Sample "T72S4" denotes control sample #4 after 72 hours of hydrolysis.

Rezex Pb column method development experiments

Exp. #	Analytes	Mobile phase	Flow rate	Temperature	Runtime	Notes
1	Sugarmix	H_2O	0.6 mL/min	75 °C	60 min	
2	Sugarmix	H_2O	0.6 mL/min	80 °C	24 min	
3	Sugarmix	H_2O	0.5 mL/min	80 °C	30 min	
4	Sugarmix	H_2O	0.8 mL/min	80 °C	20 min	
5	Sugarmix	0.4v% MeOH	0.6 mL/min	80 °C	24 min	
6	Sugarmix	0.4v% MeOH	0.6 mL/min	80 °C	24 min	
				70 °C		
				60 °C		
7	Sugarmix	4v% MeOH	0.6 mL/min	80 °C	24 min	
8	Sugarmix	H_2O	0.6 mL/min	80 °C	24 min	
	Glucose					
	Xylose					
	Mannose					

	Rhamnose					
	Arabinose					
	Galactose					
	Ethanol					
	Glycerol					
9	Sugarmix	H_2O	0.6 mL/min	80 °C	24 min	
10	Sugarmix	H_2O	0.6 mL/min	80 °C	24 min	
	Ethanol					
	T72S4				60 min	*
11	Glucose	H_2O	0.6 mL/min	80 °C	24 min	**
	Xylose					
	Mannose					
	Rhamnose					
	Arabinose					
	Galactose					
	Ethanol					
	Glycerol					
12	New Sugarmix	H_2O	0.6 mL/min	80 °C	24 min	**

* Diluted 1:4. ** Diluted in binary series from 1:1 to 1:64.

Table 15 - Overview of the experiments conducted for the method development on the Rezex ROA column for detection of inhibitors and sugars on the gradient HPLC. All samples were run with 5 mM H_2SO_4 as a mobile phase, a flowrate of 0.8 mL min^{-1} at 80 °C and were detected with PDA detector at 240, 230, 220 and 210 nm. All samples were also run isocratically. Sample "T72S4" denotes control sample #4 after 72 hours of hydrolysis.

Rezex ROA column method development experiments

Experiment	Analytes	Dilution factor	Runtime
1	Sugarmix	1	20 min
	Acid mix		
	Aromatics mix		120 min
2	HMF	2	40 min
	Furfural		
3	Sugarmix	1	20 min
	Acid mix		
	Aromatics mix		120 min
4	Citrate	2	15 min
	Formic acid		
	Acetate		
	Levulinic acid		
	HMF		40 min
	Furfural		
5	T72S4	4	95 min
	Sugarmix	1	20 min

Sugar recovery standards for total carbohydrate analysis

Table 16 – The CVS recovery rate for the five different sugars identified in the total carbon analysis of the solid fraction. The measured concentration is that which was reported by the IC analysis while the standard concentration is the actual concentration of the standards.

Standard	Measured conc. gL^{-1}	Std. conc. gL^{-1}	%CVS recovery
Mannose recovery standard	0.483	0.340	141.93%
Galactose recovery standard	0.172	0.173	99.71%
Glucose recovery standard	1.19	1.384	85.94%
Xylose recovery standard	0.140	0.208	67.57%
Arabinose recovery standard	0.114	0.092	124.05%